EVALUATING MORPHOLOGICAL DIFFERENCES BETWEEN TWO MICROBIAL MAT MORPHOTYPES FROM LITTLE AMBERGRIS CAY AS A TOOL FOR STUDYING THE GEOLOGICAL RECORD

by
Sydney Riemer

Undergraduate Thesis

Advisor: Dr. Maya Gomes

Department of Earth and Planetary Sciences, Johns Hopkins University

April 20, 2018

Abstract

Fossilized microbial mats are important records of early life on Earth. The changing macroscale morphology of these lithified microbial mats through time has been interpreted as either the result of biological evolution or changing environmental conditions. Microbial mats from active carbonate platforms serve as modern analogues and possible precursors to lithified microbial mats, thereby allowing us to test hypotheses about microbial mat formation, growth, and morphology. In this study, we apply geological methods used to study the sedimentary record of ancient microbial mats to two modern microbial mat morphotypes–the polygonal and flat mats–from Little Ambergris Cay, Turks and Caicos Islands. We investigate the upper pigmented layers of these mats, and the buried layers that represent previous generations of surface microbial mat communities. Using scanning electron microscopy, we obtain point counts of mat taxa and widths of mat cyanobacteria. We find that filament widths between the polygonal and flat mats are indistinguishable, and that the filament widths and microfaunal abundances of the lower layers of the active mats are similar to the old mats. In addition, we document differences in microfaunal abundances and filament widths between the surface layers and old counterparts of the polygonal and flat mats, indicating environmental changes through time. These results imply that mat morphologies are influenced by environmental conditions rather than microbial communities, and are consistent with findings from gene sequencing studies. Overall, the results of this study demonstrate that distinct mat morphologies occur not because of biological diversity, but environmental factors and have implications for studying paleoenvironmental change in sedimentary records of lithified microbial mats.

1. Introduction

1.1 Microbial Mats and Stromatolites

The geological record is a useful archive of the co-evolution of life and the environment, yet can be difficult to interpret due to the post-depositional alteration of rocks and sediments by tectonic activity and diagenesis, which distort paleoenvironmental records. Therefore, when studying the geological record, it is helpful to look at modern systems that may serve as analogues to the geologic feature being studied. One such geologic feature that has benefited from studies of modern analogues are stromatolites, often interpreted to be lithified microbial mats. Stromatolites are present in some Archean rocks, become ubiquitous in shallow marine Proterozoic sediments, and then decline at the start of the Phanerozoic (Peters et al., 2017). Stromatolites are formally defined as attached, lithified sedimentary growth structures, accretionary away from a point or limited surface of initiation. They are also distinctively layered, with individual laminae representing incremental growth of the microbial mat over time as sediment is accreted (Grotzinger and Knoll, 1999), although they can also grow by abiotic processes (Grotzinger and Rothman, 1996). The two commonly accepted mechanisms for microbially-mediated stromatolite growth and accretion are: (1) the trapping and binding of sediments in microbial mats and (2) the precipitation of carbonates and other inorganic materials through the activity of microbial mats (Grotzinger and Knoll, 1999). Stromatolites are significant because they can be archives of ancient organisms, ecosystems, and environments on the early Earth and throughout geologic time. However, both biological and environmental processes influence stromatolite forms found in the geological record. Yet, diagenetic alteration of rocks makes it difficult to identify the taxonomic and metabolic diversity of microorganisms found in stromatolites (Knoll et al., 2013). This leads to the question of whether variations in stromatolite form are due to the evolution of mat-building microorganisms or changing environmental conditions. Thus, there is the potential to uncover important information on biological evolution and global environmental change from morphological signatures in stromatolites. Here, I present a study of modern microbial mats as potential stromatolite precursors in order to evaluate the biological and environmental factors that influence microbial mat–and possibly also stromatolite–formation, growth, and morphology.

Microbial mats are multilayered structures of microorganisms across all three domains of life with diverse lifestyles and metabolisms. Microbial mats also contain the metabolic byproducts of these microorganisms as well as trapped sediments, mineral precipitates, and allochthonous material (Des Marais, 2003). They are found all over the Earth in environments ranging from Antarctic lakes to the deep sea. Microbial mats typically adhere to a pattern of vertical stratification. The two layers found in most mats exposed to light are a green layer and a pink layer. The top green layer is typically on the mm- to cm- scale and is host to photoautotrophs and heterotrophs. Of these, the most important for mat-building are photosynthetic cyanobacteria (Knoll et al., 2013). In the pink layer below the green layer, light penetrates but oxygen does not because it is consumed in the top green layer. Therefore, this layer is host to anoxygenic photoautotrophs such as purple sulfur bacteria that give this layer its pink color and use H_2S rather than H_2O for photosynthesis, as well as anaerobic heterotrophs and chemoautotrophs. Microbial mats accrete upward over time, and material and biomass in the upper layers becomes substrates for heterotrophs in the lower layers. The lower layers of the mats are typically brown in color and consist of degraded and decomposed biomass of past upper-mat layers. The material in the lower brown layers is the material that has the potential to

enter the geologic record. This vertical stratification pattern is important to consider because modern microbial mats serve as analogs to those preserved in the geologic record, and therefore we can compare what diversity we see in the surface layers of modern microbial mats to the lower layers that contain previous generations of the mats to learn what aspects of biodiversity are preserved in lithified microbial mats. Thus, microbial mats in carbonate environments offer insights into the physical, chemical, and biological processes that occur as these diverse ecosystems go through various stages of degradation and decay during burial, and how these various processes affect mat structure and stromatolite formation.

1.2 What aspects of Earth history do lithified microbial mats record?

Lithified microbial mats occur as a variety of morphological forms and fabrics that change both temporally throughout geologic time and spatially with depositional environment. Common stromatolite morphologies include stratiform, domal, columnar, and coniform (Knoll et al., 2013). It is inferred that stromatolite macrostructure is ultimately influenced by the shape and relief of the lamina, and therefore it is the microstructural characteristics of stromatolites that are studied to determine how different stromatolite morphologies originate. Microstructural characteristics that are often studied include cyanobacterial filament orientation, size and shape, and inorganic-precipitate fabric (Knoll et al., 2013; Grotzinger and Knoll, 1999). Though stromatolites have been studied for over a century, it is still unclear what processes are most important in influencing microbial mat and stromatolite morphology. Elucidating this can help researchers determine what components of stromatolite morphology represent information about biological diversity and evolution, global and local environmental change, or both.
Researchers have come at the stromatolite morphogenesis problem from a variety of angles using different methods and techniques. Grotzinger and Knoll (1999) use numerical simulations to argue that changing stromatolite morphology over time is a result of changes in the saturation state of seawater carbonate. The changing carbonate saturation state of seawater then determines whether stromatolites will form by trapping and binding of sediments or in-situ precipitation of carbonate, two stromatolite formation mechanisms that result in different morphologies (Grotzinger and Knoll, 1999).

Another study made observations of Proterozoic stromatolites from the Angmaat Formation in Canada, which records intertidal to supratidal carbonate deposition (Knoll et al., 2013). They found stromatolites of varying morphologies there, and by analyzing which microfabrics are correlated with different microfossil assemblages, they determined that stromatolite microfabrics and therefore macro-morphology vary depending on whether the mat is composed of mostly coccoid bacteria, vertically oriented cyanobacteria filaments, or both horizontally and vertically oriented filaments. As a result, their conclusion was that microstructural fabrics of stromatolites, and therefore also morphology, are influenced by the microbial populations. Filament orientation is also one of the characteristics most influential to the structure. Additionally, they showed that stromatolites with the most diverse microfossil populations occur in depositional environments where they are more frequently submerged, and that those with less diverse populations occur in environments where there is more subaerial exposure. Therefore, to some extent, environmental conditions also affect stromatolite structure. The modern microbial mats in this study occur in intertidal environments and can be used to test the effect of water depth on mat diversity, though not to the same extent as Knoll et al. (2013) because of the less extreme change in water depth.

With the development of genomics and gene sequencing, researchers can now obtain a more accurate estimate of the identity and diversity of microbial populations in microbial mats. Because many microorganisms, especially cyanobacteria, have morphological features that may seem to distinguish species, but which are homoplastic, gene sequencing is crucial for the taxonomic classification of microbial mat organisms (Trembath-Reichert et al., 2016). A recent study from Little Ambergris Cay, Turks and Caicos Islands, the same field site from this study, used 16S rRNA gene sequencing and compared the cyanobacterial and non-cyanobacterial populations of two microbial mat morphotypes to test the hypothesis of whether microbial population affects mat morphology (Trembath-Reichert et al., 2016). Notably, the mat morphotypes they chose for their study are the polygonal and flat mats, the same morphotypes used in this study. They found that while cyanobacteria are responsible for the structural components of both mat types, the cyanobacterial populations of the two mats are essentially the same, indicating that it is not the taxonomic classification and diversity of the primary mat-builders that influences mat morphology. The study did find that there are significant differences in the non-cyanobacterial populations of the two mat types, and that the mat type found in the interior of the lagoon where there is less hydrodynamic variability (polygonal mat) is more diverse than the mat type found closer to the main tidal channel that has more hydrodynamic activity and disturbance happening around it (flat mat). Lastly, Trembath-Reichert et al. (2016) hypothesized that the polygonal mat morphology might develop from an initially flat mat morphology, where diversity increases over time when there is little environmental disturbance to the mat. This hypothesis was based on previous work from Wanless et al. (1988) that categorized the mat morphotypes based on the presence of cyanobacteria with different colonization strategies. The flat mat had a "Schizothrix" morphology that was described as a rapid colonizer whereas the polygonal mat had a "Scytonema" morphology that was slower growing and colonized areas that were previously covered by "Schizothrix." Trembath-Reichert et al. (2016) combined this finding with conclusions from other studies on modern stromatolites that showed that hydrodynamics and sedimentation were important factors controlling morphology (Andres and Reid, 2006). Therefore, they concluded that mat morphology is influenced by environmental conditions, in this case environmental disturbances such as sedimentation and erosion due to storms or proximity to tidal channels.

1.3. Objectives and Hypotheses

The purpose of this study is to use modern microbial mats with distinct morphologies to evaluate differences between the microbial populations of the two mats types, and what aspects of these differences might enter the geological record and yield information about either biological evolution or environmental change. In order to do so, I investigate microfaunal assemblages in two microbial mat morphotypes from Little Ambergris Cay, Turks and Caicos Islands, British Overseas Territories to test hypotheses about biological and environmental influences on microbial mat morphology, as well as the potential preservation of these mat communities in the geological record. Little Ambergris Cay is a carbonate platform where sediment fluxes are limited (Gomes et al., *in revision*). Therefore, the microbial mats on Little Ambergris Cay are not lithified and also do not participate in much sediment trapping or binding. This allows us to observe how the physical, chemical, and biological processes at play in the system affect mat morphology before lithification. It also enables us to view the mat microstructures without the distorting influence of lithification or sediment trapping. This makes

Little Ambergris Cay mats particularly useful for testing hypotheses on the processes of degradation and decay that influence what stromatolites in Precambrian carbonates record.

Microbial mats on Little Ambergris Cay, like Precambrian stromatolites, occur as a variety of morphotypes. The three observed morphotypes are classified based on texture and morphology, and vary with elevation (Stein et al., 2016). The mat type occurring at the lowest elevation is the permanently submerged extracellular polymeric substance (EPS) coated flat mat. The polygonal mats with tufts of cyanobacterial sheaths are tidally submerged, and the blister mats are only submerged during storms (Fig. 1; Stein et al., 2016). This study considers the EPS-coated flat mats and tufted polygonal mats because they are the two most common types of mats on the Caicos platform (Trembath-Reichert et al., 2016) and can be used to test hypotheses about mat morphology and water depth.

In this study, one flat mat and one polygonal mat were sampled, and sections were taken of the green and pink layers of both mats and imaged using scanning electron microscopy (SEM). Samples from the lower brown layers that represent buried surface layers were also taken and imaged, because while it is important to look at the upper, live mat layers, the lower old mat could also be representative of what might enter the geological record. By comparing the old layers to the upper layers of the active mat, we can see what information is lost upon decay and degradation of the mat and what preservational biases there may be. Imaging software (JMicroVision 1.2.7) was used to do point-counts of mat features and organisms and make measurements of bacteria filament widths. Though it was shown using 16S rRNA gene sequencing that the polygonal mats are taxonomically more diverse than the flat mats, (Trembath-Reichert et al., 2016), researchers studying lithified microbial mats in the rock record do not have the ability to use gene sequencing to determine which microbial species are present and how diverse the population is. Instead, many studies of lithified microbial mats and microbial fossils in general use microfossil morphology as a way to differentiate between taxa such as coccoidal vs. filamentous bacteria, and filament width as an indicator of species, specifically when it comes to cyanobacteria (Mackey et al., 2015; Knoll et al., 2013; Boal and Ng, 2010; Schopf, 1993; Shixing and Huineng, 1992; Barghoorn and Tyler, 1965). Therefore, measuring filament width rather than using genomics in the modern mat samples across the two morphotypes can allow us to test if their cyanobacterial populations have similar morphological characteristics, while obtaining a result that may be more useful and have more application for geological studies of ancient microbial mats. Statistical analyses were performed in Python on the point-count and filament width data to test hypotheses about how mat macrostructure provides information about microbial communities and/or environmental conditions and how this information might be recorded in the geological record.

A few different hypotheses were tested using point-count data of mat microorganisms and filament width data of probable cyanobacteria. First, based on the morphological diversity of organisms, we determine what morphological differences there are overall between the two mats. Next, we determine if the cyanobacteria population of the polygonal mat is indistinguishable from that of the flat mat based on the widths of the cyanobacteria filaments. Finally, we determine if the old, buried polygonal and old flat mats have any similarity to either the active polygonal and flat mats or each other, and the significance of this for the flat to polygonal mat succession hypothesis as well as paleoenvironmental analysis. Overall, we aim to understand the potential of morphological signatures in extant microbial mats to provide information about ancient microbial mat ecosystems and/or environmental conditions.

2. Methods

2.1 Study site

Little Ambergris Cay is an uninhabited island on the Caicos Platform with an area of about 6 km x 1.6 km (Fig. 2). It is at an elevation of 1-1.5 m above sea level and is framed by a bedrock rim of oolitic grainstone (Gomes et al., *in revision*; Orzechowski et al., 2016; Stein et al., 2016). The interior basin of the island is dominated by microbial mats and mangroves (Stein et al., 2016). Water depth varies tidally by up to 50 cm, although this variability is less in the island interior. The microbial mats in the shallow bays and channels of the island interior vary in morphology with elevation and water depth (Gomes et al., *in revision*). The polygonal mats occur as discrete quasi-polygons while the flat mats are laterally continuous (Fig. 3).

The polygonal and flat mats used for this study were sampled in July 2016 and August 2017. The polygonal mat, sample CC17-4, was collected on August 4, 2017 (Fig. 3 and 4). The top pigmented layers of CC17-4 contain a 5 mm thick surface layer of dark green tufts, followed by a 1 mm lighter green-white layer that contains calcium carbonate grains, a 2 mm green layer with filaments, and lastly, a 2-4 mm pink layer. Beneath these layers are alternating layers of brown, filamentous layers and ooid layers (Fig. 4). The flat mat, sample CC3, was collected on July 4, 2016 (Fig. 3 and 5). The top pigmented layers of CC3 are a 2-3 mm thick, grainy lime green layer followed by a 1 mm pink layer (Fig. 5). The unpigmented layers are brown, filamentous and granular layers. The mats were stored in plastic bags and refrigerated until sectioning for microscopy. In this study, the top pigmented layers and a section of older material from the unpigmented layers were studied for both mat morphotypes. Representative SEM images of all four mat samples are shown in Figure 6.

2.2 Scanning electron microscopy

Scanning electron microscopy (SEM) was chosen as the imaging technique because it allows us to view the structure of the mat and the relative positions of its components, which is useful for obtaining structural information such as filament orientation. SEM sample processing requires sectioning and fixing the mat samples in order to obtain the best quality images. For the polygonal mat, one ~3 cm thick section of the green and pink pigmented layers was taken for imaging as well as one ~2 cm thick section of a brown filamentous layer starting from ~4 cm deep in the mat. This layer was chosen because there were visible vertical tufts, and because it occurs deep enough in the mat that we can observe an entirely different generation of mat growth. This allows us to test hypotheses about microbial mat succession after storm or other disturbance events as well as what from the active polygonal mat might be preserved in the degraded polygonal mat that could enter the geologic record. From the flat mat, one ~2 cm thick section was taken of the green and pink pigmented layers and one ~2 cm thick section of a tan layer from ~4.5 cm deep in the mat was taken to again test hypotheses about preservation in the geologic record. The unpigmented layers represent the old, buried mats that contain material that might enter the geological record while the pigmented, active layers capture the processes that occur before degradation, decay, and possibly lithification. Prior to sectioning, a sterilized razor blade was used to remove all material that had come into contact with the plastic bag. Sterilized razor blades were used for the carving and removal of the individual sections from the mats. Fixation of the mat is necessary so that the electron beam in the SEM does not destroy the sample and render it unavailable for further use. The fixation protocol followed in this study is the protocol followed at the Integrated Imaging Center at Johns Hopkins University (IIC), where

all sample preparation and imaging took place. All four mat sections were fixed with 3.0% formaldehyde and 1.5% glutaraldehyde in 0.1 M sodium cacodylate and 5 mM Ca^{2+}, 5 mM $MgCl^{2+}$, 2.5% sucrose, pH 7.4, at room temperature for one hour. Samples were then washed three times in 0.1 M cacodylate, 2.5% sucrose, pH 7.4, for fifteen minutes for each wash. Afterwards, samples were post-fixed with Palade's OsO_4 for one hour in the dark. 5 mL of Palade's 1% OsO_4 is composed of 1 mL Acetate-veronal sock, 1.25 ml 4% OsO_4, 1 ml 0.1 N HCl, and 1.75 ml deionized water. After osmication the mat samples become discolored and it is difficult to tell with certainty what was the original "up" direction. Therefore, 0.10 mm stainless steel minutien pins were embedded into the top layers of all samples before fixation in order to preserve the original orientation. After the fixation process, samples were immersed in ethanol and dried using a Tousimis 795 critical point dryer. After samples were dried they were mounted on SEM stubs and sputtered with platinum in an Anatech Hummer 6.02 Sputter Coater. The processed samples were then kept in SEM stub boxes until imaging.

All SEM imaging was done on the FEI Quanta 200 Environmental SEM at the IIC. For each of the active and old polygonal mat sections and each of the active and old flat mat sections, twenty sites were sampled for imaging at intervals of roughly every 1-3 mm. Images were taken from both the green and pink layers of the active mats. Two images were taken at each site, one at ~1000x and another at around ~3500x. Images were taken at these two magnifications in order to reduce bias towards either large or small organisms and features. High voltage mode was used for all images. In all subsequent sections, discussion of the polygonal mat and flat mat refer to the combination of results and analysis from both the green and pink layers of those mats.

2.3 Image analysis

All SEM images were analyzed using the image processing software JMicroVision. For each of the two images taken at the twenty sites from the four mat sections, 100 counts of mat organisms and features were done using the random point counting tool in JMicroVision. Widths were taken for cyanobacteria and bacteria filaments that were identified during point counting using the spatial calibration and 1D measurement tools.

2.4 Statistical methods

Different statistical methods were employed using Python for analyzing the point count data and the filament width data. In order to analyze the point count data of the various features and species/morphologies in the mats, two statistical methods were used to help visualize and quantify the data. First, to visualize differences between the polygonal, flat, old polygonal, and old flat mats, principal component analysis (PCA) was applied to the data in a variety of different ways to investigate relationships in the data. Across the four different mat samples, nine different microorganism morphologies and features were identified during point counting. The relative abundances of these features were then calculated. The most abundant of these features by far was amorphous organic matter, the classification used for the decayed and featureless organic matter in the mats. In order to explore how similar the mats are based on both the whole sample and identifiable organisms present, PCA analysis was done on the point count relative abundance data with and without amorphous organic matter. Additionally, a third PCA analysis was done on the data with the removal of singletons and other non-organismal features that were observed. Doing these multiple PCA analyses allows for the data to be analyzed in different ways to see how the mats are similar or different in terms of their organisms present as well as other identifiable features that may affect mat structure and morphology.

The second statistical method used to analyze the point count data and determine how similar the different mat samples are to one another was non-metric multidimensional scaling. The Bray-Curtis dissimilarity metric is commonly used in ecology to evaluate the dissimilarity between two different sites. The Bray-Curtis dissimilarity metric was chosen for this study because it can be used on relative abundance data from different locations, or in this case, different microbial mat types and ages. The Bray-Curtis dissimilarity metric returns a percent dissimilarity between two mat types and/or layers (e.g. percent similarity between polygonal and flat mats, or percent similarity between the polygonal green layer and the polygonal pink layer) that can be used to determine how similar the mat types and layers are relative to one another by looking at the percent similarity, which is 1-percent dissimilarity. Because all mat types and layers have a >83% relative abundance of amorphous organic matter, Bray-Curtis dissimilarity analysis was carried out on the relative abundances including amorphous organic matter and normalized without it in order to obtain a better estimate of the differences between the microbial populations. Absolute abundances of microfauna and features counted using point counting and analyzed by PCA and Bray-Curtis dissimilarity are in Table A1.

For the filament widths, the Welch's t-test, or the unequal variances t-test, was used to test the hypothesis that that the cyanobacteria filament widths in the polygonal mat are indistinguishable from those in the flat mat. The Welch's t-test was also used to determine if the cyanobacteria filament widths are indistinguishable between the old mat samples and the active mat samples in order to help determine if the old samples represent buried polygonal or flat mats. The Welch's t-test was used because of the differing variances and sample sizes of filament widths from the different mat types and layers (Table A2). Because Welch's t-test assumes normality, the test was performed on filaments with widths from 0-5 μm, a range where the data are approximately normal. However, Welch's t-test is robust to non-normality (Ruxton, 2006), allowing the test to be performed on the whole range of filament width data as well. Therefore, Welch's t-test was carried out on different combinations of comparisons for the mat samples, and t-statistics and p-values were obtained to determine whether or not filament widths between the mat samples are significantly similar. All analyses including Welch's t-test, PCA, and Bray-Curtis dissimilarity were performed using the Python programming language's SciPy statistical packages and their functions (Welch's t-test: scipy.stats.ttest_ind; PCA: sklearn.decomposition.PCA; Bray-Curtis dissimilarity: scipy.spatial.distance.braycurtis). See the SciPy documentation for more information on those functions.

3. Results

3.1 Point counting

The most abundant mat morphology/feature identified during point counting across all four mat samples was amorphous organic matter, which accounts for >83% of features observed in the mats (Fig. 7 and 8). The polygonal mat and its green and pink layers have both the least amorphous organic matter and the most cyanobacterial filaments. The old mats have the most amorphous organic matter, though the flat mat has a similar relative abundance of amorphous organic matter as the old polygonal and old flat mats (Fig. 7 and 8). The other features/taxa identified in the mats are cyanobacterial filaments, other bacterial filaments (bacterial filaments that aren't obviously thick cyanobacteria filaments and therefore could be other bacterial taxa), coccoidal bacteria, colonial coccoidal bacteria, diatoms, eukaryote feces, dinoflagellates, and larval mollusks.

Removing amorphous organic matter and renormalizing the relative abundances of the mat features and taxa makes it easier to see the abundances of identifiable microfauna (Fig. 9 and 10). Therefore, all subsequent discussion of results refer to those analyses that were done without taking into account amorphous organic matter, unless specified. The top three most abundant microfauna across all four mats are bacterial filaments, cyanobacterial filaments, and coccoidal bacteria. Colonial coccoids and diatoms are also relatively significant in the polygonal, flat, and old flat mats. Diatoms make up a significant fraction of the microfauna in the flat mat and are also present in the polygonal mat and the old mats. Although diatoms would not be present in Precambrian stromatolites because of their evolution later in the Phanerozoic, they are a significant component of the Little Ambergris Cay microbial mats, and therefore were kept in the analyses. The polygonal green layer has the most cyanobacterial filaments, which account for ~42% of that mat layer. The flat mat has the least amount of cyanobacteria filaments. The other mat features occur as singletons or are non-microbial (Fig. 9 and 10). The polygonal, flat, and old flat mats have seven different identifiable taxa, whereas the old polygonal mat only had six distinct features.

PCA analyses were carried out on the relative abundance data in three permutations; (1) with amorphous organic matter, (2) normalized without amorphous organic matter, with singletons and non-microbial features, and (3) normalized without singletons and non-microbial features. The removal of the amorphous organic matter and singletons is justified here because when studying the geological record, researchers often only take into account the identifiable morphologies. Similarly, researchers studying fossil microbial mats would be able to observe singletons and handle them in their analyses. PCA analyses were used to visualize similarities between the bulk mats, as well as the individual mat layers. For PCA carried out on the bulk mats and individual layers with amorphous organic matter, the flat mat and the old polygonal mat plot close to each other, indicating their similarity (Fig. 11a,b). On the individual-mat-layer level, the old polygonal mat and the flat mat pink layer plot close to one another, which is consistent with what was observed in the PCA plot for the bulk mats (Fig. 11b). When the analysis is done without taking into account the relative abundance of amorphous organic matter, the results are slightly different. On the bulk mat level, none of the mats plot close to one another, though the flat mat and the old polygonal mat plot relatively close (Fig. 11c). On the other hand, for the individual mat layers, the flat mat pink layer and the old polygonal mat still plot close together like they did for the analysis done including amorphous organic matter (Fig 11d). Next, PCA was done on the data without singletons, and with and without amorphous organic matter. For the bulk mat data, none of the mats plot close to each other for the analysis done both with and without amorphous organic matter (Fig. 12a,c). However, for the individual mat layer analyses with and without amorphous organic matter, the old polygonal mat and the flat mat pink layer plot close to each other like they did in the analyses including the singletons and non-microbial features (Fig. 12b,d). A new relationship emerged in the analysis without singletons and without amorphous organic matter between the old flat mat and the polygonal mat pink layer, which plot close to one another (Fig. 12d). Overall, the mat types and layers that show similarity in their taxa and features based on PCA are the old polygonal mat and the flat mat, the old polygonal mat and the flat mat pink layer, and the old flat mat and the polygonal mat pink layer.

In order to quantify the similarity between the mat types and layers based on relative abundance of taxa and other features obtained from point counting, the Bray-Curtis dissimilarity metric was used. The Bray-Curtis dissimilarity analysis was done without considering

amorphous organic matter. Note that numerical data in Figures 13 and 14 are the percent similarity between the mat types and layers, where percent similarity=1-percent dissimilarity and multiplied by one hundred. For these analyses all percent similarities are >50%. For the analysis done using relative abundances on the bulk mats, the flat and old polygonal mats have the highest percent similarity (90.4%), a result that is consistent with PCA, and the polygonal and old flat mats have a similar percent similarity (89.3%) (Fig. 13). The old polygonal and the old flat mats also have a similar percent similarity, at 86.6%. The polygonal and the old polygonal mats, and the flat and the old flat mats, have percent similarities of 76.4% and 80.5%, respectively (Fig. 13). The least similar mats based on point count data are the polygonal and the flat mats.

Lastly, the Bray-Curtis analysis was performed on the individual mat layers to see how similar they are to each other and the old mat layers (Fig. 14). The comparisons with the highest percent similarity are the polygonal pink layer and the old flat mat (92.7%), the polygonal pink layer and the old polygonal mat (89.3%), and the flat mat pink layer and the old polygonal mat (87.9%). The latter is a result that is consistent with PCA. The least similar layers were the polygonal green and flat green layers, and polygonal green and flat pink layers. The flat green layer and old flat mat, and the polygonal green layer and old polygonal mat also have relatively low percent similarities. Another notable comparison is the polygonal pink and flat pink layers (83.7%). All other comparisons are shown in Figure 14. The results obtained from the Bray-Curtis dissimilarity metric are mostly consistent with the results from PCA and allow us to quantify the relative similarities between the different mat types and their layers.

3.2 Filament widths

Across all mat types and layers, bacterial filament widths ranged from less than 1 μm to 70 μm. Thin filaments are defined here as filaments less than 10 μm, and typically ranged from 0-5 μm. Thick cyanobacterial filaments ranged from 10-70 μm. Of the polygonal, flat, old polygonal, and old flat mats, the polygonal mat has the thickest filament widths, with an average filament width of 7.89 μm (Table A2). The flat mat has the thinnest filament widths, with an average filament width of 3.27 μm (Table A2). Of the green and pink layers in the polygonal and flat mats, the polygonal green layer had the highest average filament width, and the flat green layer had the lowest (Table A2). The number of filament widths measured, their mean, standard deviation, and variance for each mat type and layer are reported in Table A2. A histogram of the filament widths across all mat types and layers is shown in Figure 15. The filament widths that were encountered at the highest frequency are those in the range from ~0-5 μm. This trend is the same at both the individual mat and layer levels (Fig. 16-19). Because of this distribution, t-tests were also performed on only the 0-5 μm filament width data (Table A3) in order to see if the mats are significantly similar in that filament width range.

Using a significance level of 0.05, from Welch's t-test across the entire filament width range the following mat filament width comparisons for the bulk mats have significantly similar widths: the polygonal and old polygonal mats, the polygonal and old flat mats, and the old flat and old polygonal mats (Fig. 20). On the individual mat-layer-level, the following have significantly similar widths: the polygonal green and polygonal pink layers, the polygonal green and pink layers and old polygonal mat, the polygonal green and pink layers and old flat mat, the flat green and flat pink layers, and the old polygonal and old flat mats. (Fig. 21). All other comparisons have significantly different filament widths across their entire filament width ranges (Fig. 20 and 21). T-statistics for the p-values in Figures 20-23 are listed in Tables A4 and A5.

For the Welch's t-test for filament widths in the range 0-5 μm, all mat comparisons have significantly similar filament widths except for the old polygonal and old flat mats, the polygonal green and polygonal pink layers, the old flat mat and the flat green layer, and the old flat mat and polygonal green layer (Fig. 22 and 23).

4. Discussion

A notable result from the PCA and Bray-Curtis dissimilarity analysis is that the pink layers of the polygonal and flat mats are more similar to the old mat layers than the green layers (Fig. 12d and 14). Although this may be surprising given that previous work has showed that thick cyanobacterial sheaths, which tend to be more abundant in the upper green layer, have a higher preservation potential than other mat components (Newman et al., 2017), recent work by Gomes et al. (*in revision)* on a polygonal mat from Little Ambergris Cay obtained results that are consistent with this result. They found that labile organic macromolecules such as lipids and polysaccharides that are abundant in the green layers of the mats are quickly degraded and depleted in the lower pink layer (Fig. 24). Those results indicate that the pink layers are already partially degraded and so are closer to what may be preserved in the geological record. Therefore, the findings here using microscopy are consistent with the results from previous organic geochemistry studies that showed that the pink layers are more degraded, and in fact almost just as degraded, as the material in the previous mats. This means that there are some aspects of microbial diversity that are erased as the uppermost layers become lower microbial mat layers. It is thus important to consider the mode and timing of lithification, as this likely has a great effect on what can be preserved (Newman et al., 2017). For instance, it has been shown that cyanobacteria can calcify and induce carbonate precipitation in microbial mats by increasing pH through the photosynthetic uptake of inorganic carbon, thereby inducing lithification in the upper layers where most cyanobacteria reside (Benezrara et al., 2014; Altermann et al., 2006). In addition to this, cyanobacterial calcification and carbonate precipitation in microbial mats is also dependent on environmental conditions such as temperature and seawater alkalinity, which can affect where and when lithification occurs (Grotzinger and Knoll, 1999; Riding, 1992). Therefore, though the lower mat layers may be more representative of what might enter the geological record in modern, non-lithifying microbial mats, this might not be true of Proterozoic microbial mats that existed when carbonate precipitation was more favorable, thereby allowing the upper layers to also have the possibility to lithify and enter the geological record. Nonetheless, other studies have shown that precipitation of carbonate is correlated with the decay of organic matter in the deeper mat layers and that the degree of calcification increases with depth in the mat (Altermann et al., 2006), making our results here still applicable throughout the geological record.

Another notable result is that the flat mat has the least amount of cyanobacterial filaments (Fig. 9 and 10, Table A1). This is surprising because it would be expected that the old mat samples, specifically the old flat mat, would have the least amount of cyanobacterial filaments due to the fact that it has gone through more degradation and decay. Yet this not what we observe. One explanation for this might be that the environmental conditions were different when the old flat mat was at the surface. For example, perhaps the water depths were lower when the old flat mat was at the surface, requiring it to adapt a strategy similar to the polygonal mats, where it used empty cyanobacterial sheaths as a sort of 'sunscreen'. In that case, the flat mat would have been a polygonal mat when the old flat layer was at the surface. Indeed, changes in the hydrology of Little Ambergris Cay have been documented after storm events (M. Gomes,

personal communication, April 2018). It is also possible that an environmental condition other than water depth was different that either allowed for better cyanobacteria preservation, or for there to be more cyanobacteria growth (e.g. nutrient levels). Testing these hypotheses would require the age of the old flat strata to be determined, as well as the stated environmental conditions at the time the old mat was at the surface.

As mentioned earlier, bacterial filament widths are one of the few properties that those who study microfossils in the geological record have to identify and classify fossilized microorganisms. Because Trembath-Reichert et al. (2016) found that cyanobacterial diversity from 16S rRNA sequencing between the polygonal and flat mats on Little Ambergris Cay are indistinguishable, we hypothesized here that we should obtain the same results using filament widths. Over the filament width range of 0-5 μm, a range that most filament widths from the mats occur in (Fig. 15-19 and Fig. A1), the filament widths between the polygonal mat and the flat mat are significantly similar (Fig. 21). This result is consistent with the result of Trembath-Reichert et al. (2016), and gives further credence to the idea that the differing morphologies of the polygonal and flat mats is not due to the difference in their cyanobacteria populations. Furthermore, the result from PCA that the polygonal mat pink layer and the flat mat pink layer are more similar to the old flat mat and the old polygonal mat, respectively, rather than to the old mat they lie directly above (Fig. 12d), is also evidence that the mats are all relatively similar in terms of their bacterial filaments and microbial populations. Showing this using filament widths rather than gene sequencing also allows us to say that filament widths can be used to observe differences, or the lack thereof, between stromatolite morphotypes.

Over the entire range of filament widths observed in the mats, the filament widths are significantly different between the polygonal and flat mats (Fig. 20). In particular, the polygonal mat has filaments with widths greater than 5 μm that do not appear in the flat mat (Fig. A1). Though this result contradicts the findings of Trembath-Reichert et al. (2016) that the cyanobacterial populations are indistinguishable between the mat types based on 16S rRNA analyses, it is possible that that study is capturing the similarity in the 0-5 μm range, which is what is guiding their conclusions. Additionally, the fact that there are more thick cyanobacteria filaments that have widths not observed in the flat mat could be consistent with the observation of Trembath-Reichert et al. (2016) that the polygonal mat's microbial population as a whole is more diverse than the flat mat's. When discussing the filaments in the 0-5 μm range, it is also important to note that there are non-cyanobacterial filamentous bacteria with filament widths in the 0-5 μm range that are being included in our filament width analyses. For example, Chloroflexi are a phylum of filamentous bacteria that occur as thin filaments and are among the most abundant taxa in both the polygonal and flat mats (Gomes et al. *in revision*; Trembath-Reichert et al., 2016). Because we cannot distinguish between cyanobacterial and non-cyanobacterial filaments based on morphology using SEM, it is unknown what part of the 0-5 μm range filaments Chloroflexi account for in this study. However, considering that the most dominant cyanobacteria species occur as thin filaments, it is valid to assume that most filaments in the 0-5 μm range actually are cyanobacteria.

Although the bacterial filaments that have widths ranging from 0-5 μm are indistinguishable between the polygonal and flat mats, it is tempting to ask how cyanobacterial diversity can be ruled out as a reason for the formation of the two morphotypes based on the differences between their thick cyanobacterial filaments. However, there is a potential environmental explanation for this observation that does not require an explanation based on biological differences between the mats. The polygonal mats occur at a higher elevation than the

flat mats and therefore have more subaerial exposure (Gomes et al., *in revision*). The uppermost portion of the mat is composed of empty cyanobacterial sheaths that contain the pigment scytonemin, which acts as a protective layer against the harmful solar UV rays (Rastogi et al., 2015; Balskus et al. 2011; Garcia-Pichel et al. 1992). The flat mat, which occurs at a lower elevation and is therefore submerged, also has a protective layer, but it is made from EPS rather than empty cyanobacterial sheaths. The polygonal mats cannot use EPS as a protective layer, because it would dry out when the mats are subaerially exposed at low tide. Considering this, the result that the polygonal and flat mats have differing filament widths above 5 μm (where the ratio of filament widths greater than 5 μm to 0-5 μm is 0.61 for the polygonal mat and 0.077 for the flat mat) and therefore possibly different cyanobacterial diversity can be explained by environmental factors, meaning that environmental factors such as elevation shape mat morphology rather than biology. The idea that the water depth the mats occur in affects their morphology was put forth in Knoll et al. (2013). However, in that study they found that stromatolite facies that occur in deeper water environments are more diverse than those that occur in shallow waters. This is the reverse of what is observed at Little Ambergris Cay, where the polygonal mats that occur at higher elevations and shallower water are more diverse than the flat mats that are permanently submerged (Gomes et al., *in revision*; Trembath-Reichert et al., 2016). Therefore, other environmental factors such as hydrodynamics and sedimentation likely play a greater role in affecting the diversity of different mat morphotypes.

The filament width data analysis also shows that the old, buried mats are more similar to the pink mat layers than the upper green layers. For the polygonal mat, the filament widths in the old polygonal mat are similar to the polygonal pink layer, but not the polygonal green layer (Fig. 21). For the flat mat layers and the old flat mat, both the green and pink layers have significantly different filament widths when compared to the old flat mat. However, over the 0-5 μm filament width range, the pink layer has significantly similar widths to the old flat mat whereas the green layer does not (Fig. 23). This means that filament widths do not change significantly as the pink mat layers transition to the deeper brown layers, either because the filaments that remain in the pink layer are more resistant to decay or because subsequent decay processes are not as effective as those in the green layer. Further, because cyanobacterial and thin bacterial filaments are by far the most abundant organisms in the mats, this trend is also observed when taking into account all the organisms of the mats (i.e. from PCA and Bray-Curtis analysis). Taken together, these observations indicate that filament widths measured in the geological record can be used to extract paleoenvironmental information from lithified microbial mats.

In terms of the flat mat to polygonal mat succession hypothesis endorsed by Trembath-Reichert et al. (2016) and others, there is not an entirely clear conclusion from this study. Each metric or analysis used to characterize the mats relative to one another gives a different result. From PCA, Bray-Curtis dissimilarity, and comparisons of 0-5 μm filament widths, it is clear that the flat and old polygonal mats have similar properties. This may be an indication that the old polygonal mat layer we sampled from could have once been a flat mat that developed after some storm or other type of disruption. This interpretation would then be a validation of the flat to polygonal succession hypothesis. On the other hand, the old flat mat shows similarity to the polygonal mat pink layer in PCA (Fig. 12d), but also shows similarities to both the polygonal and flat mats using the Bray-Curtis dissimilarity metric, though it is overall more similar to the polygonal mat. Therefore, these results could just be another indication that the mats really are similar in terms of the morphologies of their biological communities, and that environment is the factor controlling macroscale mat morphologies. However, overall we have showed that the old

mats are not entirely the same as their active counterparts–an indication that these results either lend validity to the mat succession hypothesis, or show that differing paleoenvironmental conditions affected the abundance and lifestyle of mat microorganisms.

The final unexpected result was the observation of ≥70 μm wide filaments in the deep layers of the polygonal mat (Fig. 17). Thick filaments have been observed in the geological record, for example in microbialites from the Angmaat Formation that contain filaments ascribed to the extant mat-building cyanobacteria *Microcoleus chthonoplastes* (Knoll et al., 2013). However, this observation of thick filaments in the deep layer laid down by previous generations of mat communities is surprising because filaments this wide were not observed in the surface layers of the polygonal mat. Two possibilities may account for this result. First, there may have been environmental conditions at the time the old polygonal mat was at the surface that were more advantageous to large (≥70 μm wide) filamentous cyanobacteria. In this scenario, environmental conditions were different when the new, active mat was collected such that they did not allow for the growth of cyanobacteria with large filament widths. The next possibility is that as the mats were buried and organic matter from decaying organisms began to accumulate, cyanobacterial filaments were covered in this material, thereby amplifying the widths we observe. This is a plausible explanation given the appearance of the cyanobacteria filaments in the active polygonal mat, which do not have much material building up on them, and the filaments from the old polygonal mat, which appear to have material that has built up over time (Fig. 25). This notion also goes back to the conclusions from Newman et al. (2017), who found that sheathed cyanobacteria can accumulate mineral veneers of up to 1 μm in thickness around their filaments. Although the Little Ambergris mats are non-lithifying, and therefore cyanobacteria filaments likely do not accumulate mineral veneers, it is not unreasonable to think that the same idea may apply to organic matter. However, 1 μm accumulation does not explain the >30 μm increase in filament widths, or the fact that this increase does not apply to the whole range of filament widths, which is what we would expect. Additionally, not all thick cyanobacterial filaments in the old mats were observed to have accumulated material, so it is still unclear how this can affect filament widths observed in these mats and the geological record. Therefore, the former hypothesis of environmental change causing different organisms to grow is the more likely explanation.

Of course, there are limitations to this study that should be addressed. First, we only have samples from two different mats from two locations, so it isn't clear what variability may exist using the methods outlined here between different mats of the same morphotype. However, the microbial diversity results indicate that the surface polygonal (flat) mat are more similar to other polygonal (flat) mats than they are to the flat (polygonal) mats, based on similarities between the surface mats and the old mats. Also, though SEM is useful for looking at the overall structure of the mats, other types of microscopy such as light microscopy may be able to yield complementary, or more information on the organisms present in the mats. Future work therefore may include obtaining more mat samples for SEM imaging, or resampling the same mats from this study and using different methods and techniques to analyze them. Another limitation of this study is that when considering the differences between the active mats and the buried mats, we did not take into account the fact that differences between them may arise because of the decay and loss of morphological signatures. Future work can include an assessment of this based on the results of taphonomic studies of Little Ambergris Cay mats such as Gomes et al. (*in revision*). Future work will also elucidate how the methods used in this study can be used in tandem with other methods available to geologists studying lithified microbial mats, such as stable isotope

analyses, to answer lingering questions. Such questions include, for instance, can lithified microbial mats record global environmental change, or only localized changes in hydrology and sedimentation? Answering these questions will enable researchers to better understand how microscopic methods can be employed to study lithified microbial mats in the geological record, and can also shed new light on data obtained in older studies. Finally, there are significant environmental and biological differences between the present day when Little Ambergris Cay mats exist and the Precambrian, when the stromatolites that we seek to better understand existed. These differences place some limits on what we can infer about stromatolites based on what we observe in modern microbial mats. For example, atmospheric oxygen concentrations would have been lower than they are today, and diatoms and other eukaryotic taxa would not have evolved yet, changing the ecosystem of the mats. However, the abundance of cyanobacteria microfossils in stromatolites and the similar shallow, coastal marine environments these ancient microbial mats occur in shows that in general, the most salient conditions were similar.

Overall, from this study we can see that paleoenvironmental conditions have the potential to be extrapolated on the basis of morphology by observing the differences between different microbial mat morphotypes. These results from modern microbial mats can be extrapolated back to the geological record and can ultimately serve to help us better interpret stromatolites and understand environmental change throughout Earth history.

5. Conclusions

In the past, the study and interpretation of lithified microbial mats in the geological record has been made difficult by the destruction and diagenetic overprinting of primary features. This has made the observation that stromatolite morphologies and textures change through time difficult to interpret. Recent studies of modern microbial mats with varying morphologies have helped to make steps towards resolving this issue, because we have tools such as gene sequencing to determine biodiversity and can directly correlate biodiversity and environmental factors with mat morphologies. In this study, we used observations of two modern microbial mat morphotypes from Little Ambergris Cay obtained from the tools that are unavailable for studying the geological record (e.g. gene sequencing) and compared those observations to the ones obtained here through microscopy, which is used by researchers studying stromatolites, to see if similar observations can be made in the geological record. By sampling from the old, buried mats, we also tried to determine if paleoenvironmental information can be obtained from these records.

Through these indirect methods we have found that the polygonal and flat mats differ in terms of their microbial assemblages and that cyanobacterial filament widths in the 0-5 μm range are indistinguishable between the two mat morphotypes, findings that are consistent with studies of the same mat types using 16S rRNA gene sequencing. Additionally, we found that cyanobacterial filament widths and microfauna assemblages in the pink layers of the active mats are more similar to the old mats than the green layers are. These findings are consistent with results that were obtained using organic geochemistry methods, which indicate that the greatest rate of degradation occurs in the green layer, and that subsequent degradation in the pink layer and lower layers is reduced.

We also found that the surface mats do not show relative similarity to their buried counterparts, suggesting that we are capturing the effects of a lack of preservation of some taxa, or varying environmental conditions through time. In addition, the surface mats are more similar to the buried counterpart of the other mat type, e.g. the flat mat and old polygonal mat are more

similar than the flat mat and old flat mat. Moreover, the active flat mat has less thick cyanobacterial filaments than the old flat mat, which is a possible indication that environmental conditions were different when the old flat mat was at the surface, and perhaps was a polygonal mat that needed to adapt differently than a flat mat. All of these observations are potential evidence for the mat succession hypothesis and/or evidence for differing environmental conditions that required different adaptations.

Though we obtained conclusive and consistent results from this study, there is still some uncertainty and gaps in our knowledge. For instance, we still need to determine if the results from this study are repeatable, and how applicable they are across other microbial mat morphotype and environment systems. Overall, based on the findings in this study, the varying macroscale morphology of microbial mats from Little Ambergris Cay is not due to differences in the populations of cyanobacteria, the primary mat builders. The differing morphology of these mats through space and time is explained by the differing environmental conditions. Because these findings are consistent with those found using the tools employed by those studying modern systems, certain paleoenvironmental information can be obtained from lithified microbial mats using microscopy. However, considerations of the macroscale morphology of lithified microbial mats is also important, as these can be more easily observed and contribute complementary knowledge. Finally, this study is a further indication that lithified microbial mats are important records of not only the appearance of cyanobacteria and other taxa, but of environmental changes and patterns throughout Earth history.

Acknowledgements

Thank you to Dr. Maya Gomes for her help in all aspects of this project and for her guidance and unwavering support throughout. Thanks also to Dr. Michael McCaffrey from the IIC for teaching me all about scanning electron microscopy and for his helpful insight and suggestions that made this project possible. Thanks to Dr. Scot Miller and Dr. Meghan Avolio for their help with the statistical methods. Finally, thank you to the JHU Earth and Planetary Sciences department for giving me this opportunity.

References

Altermann, W., Kazmierczak, J., Oren, A. and Wright, D.T., 2006. Cyanobacterial calcification and its rock-building potential during 3.5 billion years of Earth history. *Geobiology*, *4*(3), pp.147-166.

Andres, M.S. and Reid, R.P., 2006. Growth morphologies of modern marine stromatolites: a case study from Highborne Cay, Bahamas. *Sedimentary Geology*, *185*(3-4), pp.319-328.

Balskus, E.P., Case, R.J. and Walsh, C.T., 2011. The biosynthesis of cyanobacterial sunscreen scytonemin in intertidal microbial mat communities. *FEMS microbiology ecology*, *77*(2), pp.322-332.

Barghoorn, E.S. and Tyler, S.A., 1965. Microorganisms from the Gunflint chert. Science, 147(3658), pp.563-577.

Benzerara, K., Skouri-Panet, F., Li, J., Férard, C., Gugger, M., Laurent, T., Couradeau, E., Ragon, M., Cosmidis, J., Menguy, N. and Margaret-Oliver, I., 2014. Intracellular Ca-carbonate biomineralization is widespread in cyanobacteria. *Proceedings of the National Academy of Sciences*, *111*(30), pp.10933-10938.

Boal, D. and Ng, R., 2010. Shape analysis of filamentous Precambrian microfossils and modern cyanobacteria. *Paleobiology*, *36*(4), pp.555-572.

Des Marais, D.J., 2003. Biogeochemistry of hypersaline microbial mats illustrates the dynamics of modern microbial ecosystems and the early evolution of the biosphere. *The Biological Bulletin*, *204*(2), pp.160-167.

Garcia-Pichel, F., Sherry, N.D. and Castenholz, R.W., 1992. Evidence for an Ultraviolet Sunscreen Role of the Extracellular Pigment Scytonemin in the Terrestrial Cyanobacterium Chiorogloeopsis sp. *Photochemistry and Photobiology*, 56(1), pp.17-23.

Gomes, M. et al., 2017. Microbial Mats on Little Ambergris Cay, Turks and Caicos Islands: Taphonomy and the Selective Preservation of Biosignatures. *Accepted to Geobiology*.

Grotzinger, J.P. and Rothman, D.H., 1996. An abiotic model for stromatolite morphogenesis. *Nature*, *383*(6599), p.423.

Grotzinger, J.P. and Knoll, A.H., 1999. Stromatolites in Precambrian carbonates: evolutionary mileposts or environmental dipsticks?. *Annual review of earth and planetary sciences*, *27*(1), pp.313-358.

Knoll, A.H., Wörndle, S. and Kah, L.C., 2013. Covariance of microfossil assemblages and microbialite textures across an upper Mesoproterozoic carbonate platform. *Palaios*, *28*(7), pp.453-470.

Mackey, T.J., Sumner, D.Y., Hawes, I., Jungblut, A.D. and Andersen, D.T., 2015. Growth of modern branched columnar stromatolites in Lake Joyce, Antarctica. *Geobiology*, *13*(4), pp.373-390.

Newman, S.A., Klepac-Ceraj, V., Mariotti, G., Pruss, S.B., Watson, N. and Bosak, T., 2017. Experimental fossilization of mat-forming cyanobacteria in coarse-grained siliciclastic sediments. *Geobiology*, *15*(4), pp.484-498.

Orzechowski, E. A., Strauss, J. V., Knoll, A. H., Fischer, W. W., Cantine, M., Metcalfe, K., Quinn, D. P., Stein, N., Gomes, M. L., Grotzinger, H. M., Lingappa, U., O'Reilly, S. S., Riedman, L. A., Trower, L., and Grotzinger, J. P., Age and Construction of Little Ambergris Cay Bedrock Rim, Southeastern Caicos Platform, British West Indies, in *Proceedings American Geophysical Union, Fall General Assembly* 2016.

Peters, S.E., Husson, J.M. and Wilcots, J., 2017. The rise and fall of stromatolites in shallow marine environments. *Geology*, 45(6), pp.487-490.

Rastogi, R.P., Sonani, R.R. and Madamwar, D., 2015. Cyanobacterial sunscreen scytonemin: role in photoprotection and biomedical research. *Applied biochemistry and biotechnology*, 176(6), pp.1551-1563.

Riding, R., 1992. Temporal variation in calcification in marine cyanobacteria. *Journal of the Geological Society*, *149*(6), pp.979-989.

Ruxton, G.D., 2006. The unequal variance t-test is an underused alternative to Student's t-test and the Mann–Whitney U test. *Behavioral Ecology*, *17*(4), pp.688-690.

Schopf, J.W., 1993. Microfossils of the Early Archean Apex chert: new evidence of the antiquity of life. *Science*, *260*(5108), pp.640-646.

Shixing, Z. and Huineng, C., 1992. Characteristics of Palaeoproterozoic stromatolites in China. *Precambrian Research*, *57*(1-2), pp.135-163.

Stein, N., Grotzinger, J. P., Quinn, D. P., Fischer, W. W., Knoll, A. H., Cantine, M., Gomes, M.L., Grotzinger, H. M., Lingappa, U., Metcalfe, K., O'Reilly, S. S., Orzechowski, E. A., Riedman, 1235 L. A., Strauss, J. V., and Trower, L., UAV, DGPS, and laser transit

mapping of microbial mat ecosystems on Little Ambergris Cay, B.W.I in *Proceedings American Geophysical Union, Fall General Assembly* 2016.

Trembath-Reichert, E., Ward, L.M., Slotznick, S.P., Bachtel, S.L., Kerans, C., Grotzinger, J.P. and Fischer, W.W., 2016. Gene Sequencing-Based Analysis of Microbial-Mat Morphotypes, Caicos Platform, British West Indies. *Journal of Sedimentary Research*, *86*(6), pp.629-636.

Wanless, H.R., Tyrell, K.M, Tedesco, L.P., and Dravis, J.J., 1988. Tidal-flat sedimentation from Hurricane Kate, Caicos Platform, British West Indies: *Journal of Sedimentary Petrology*, v. 58, p. 724–738.

Figures

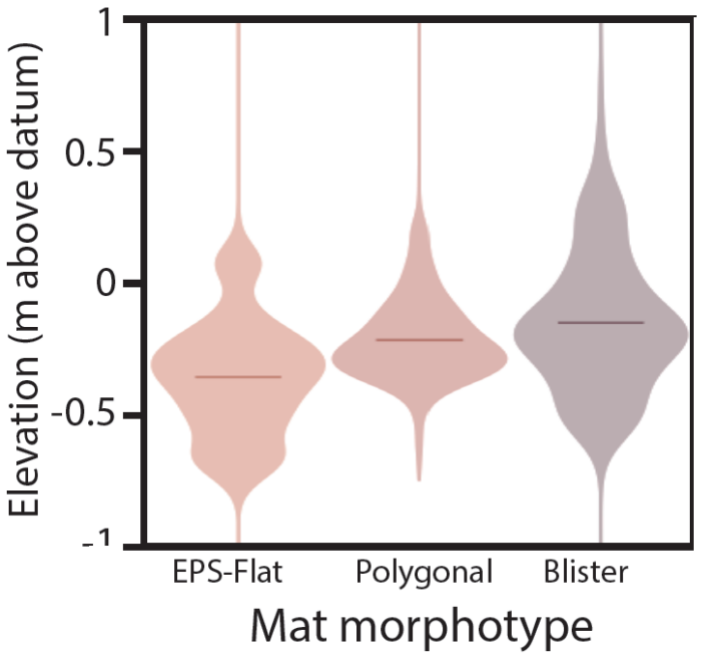

Figure 1. "Violin plot" from Stein et al. (2016) showing that the EPS-coated flat mats occur at the lowest elevations, the polygonal mats at intermediate elevations, and the blister mats at the highest elevation. Low elevation correlates with greater water depth and high elevation correlates with shallower water.

Figure 2. Location of Little Ambergris Cay within the Caicos Platform (left) and location of Turks and Caicos within the southwest north Atlantic Ocean (left, inset). The location of microbial mat study sites on Little Ambergris Cay (right) show where the polygonal mat (CC17-4) and flat mat (CC3) were sampled from. Figure used with permission from M. Gomes.

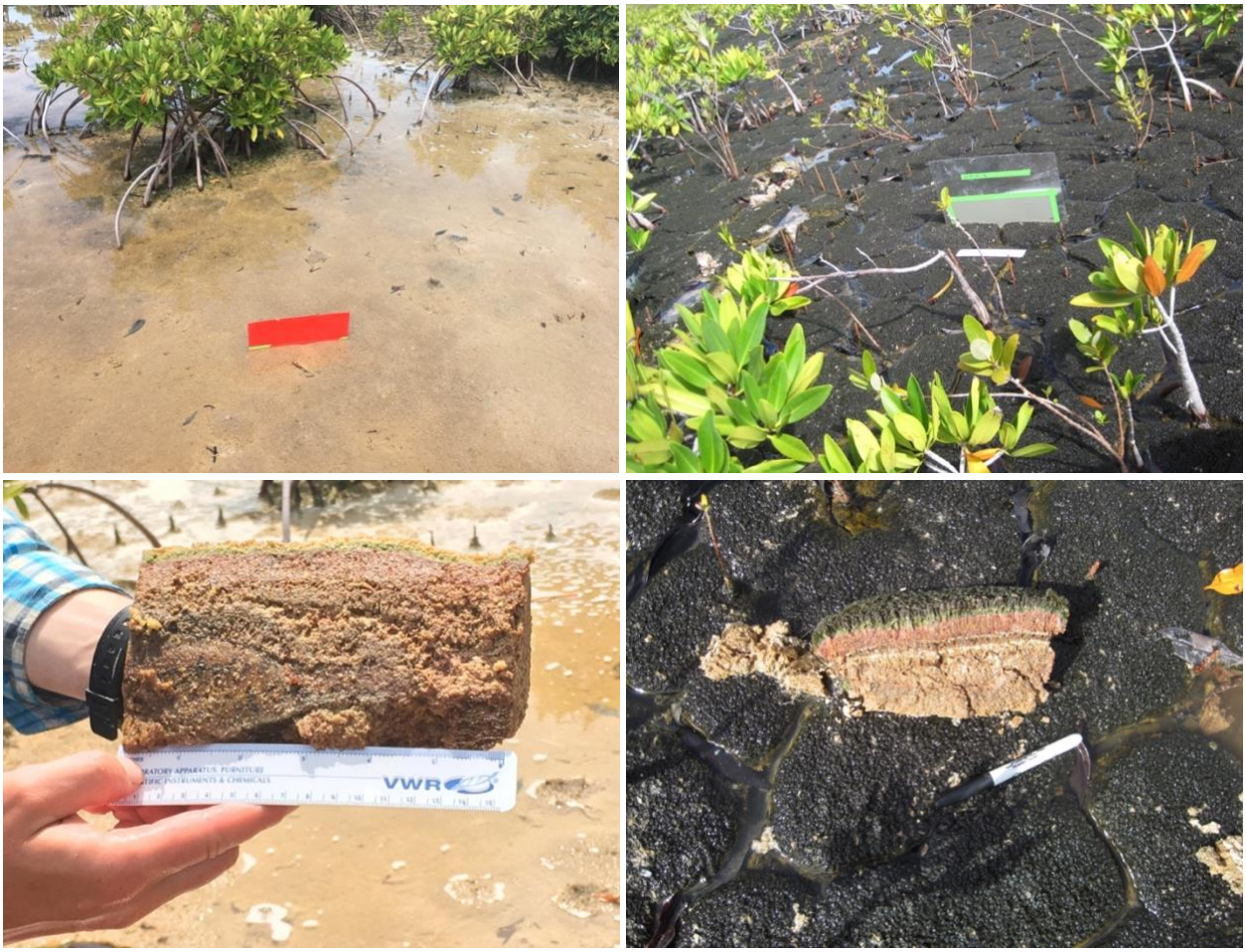

Figure 3. Images of the flat and polygonal microbial mats from Little Ambergris Cay. Top left: EPS-covered flat mats; Bottom left: vertical cross section through CC3 showing the green, pink, and old brown layers; Top right: tufted polygonal mats; Bottom right: vertical cross section through CC17-4 showing the green, pink, and old brown layers; Photo credit: Maya Gomes.

Figure 4. Cross section of polygonal mat CC17-4 showing the notable mat layers: G-green, P-pink, O1-ooid layer 1, O2-ooid layer 2, OP-old polygonal mat. Note the filamentous texture of OP. Layers G, P, and OP are the subjects of this study.

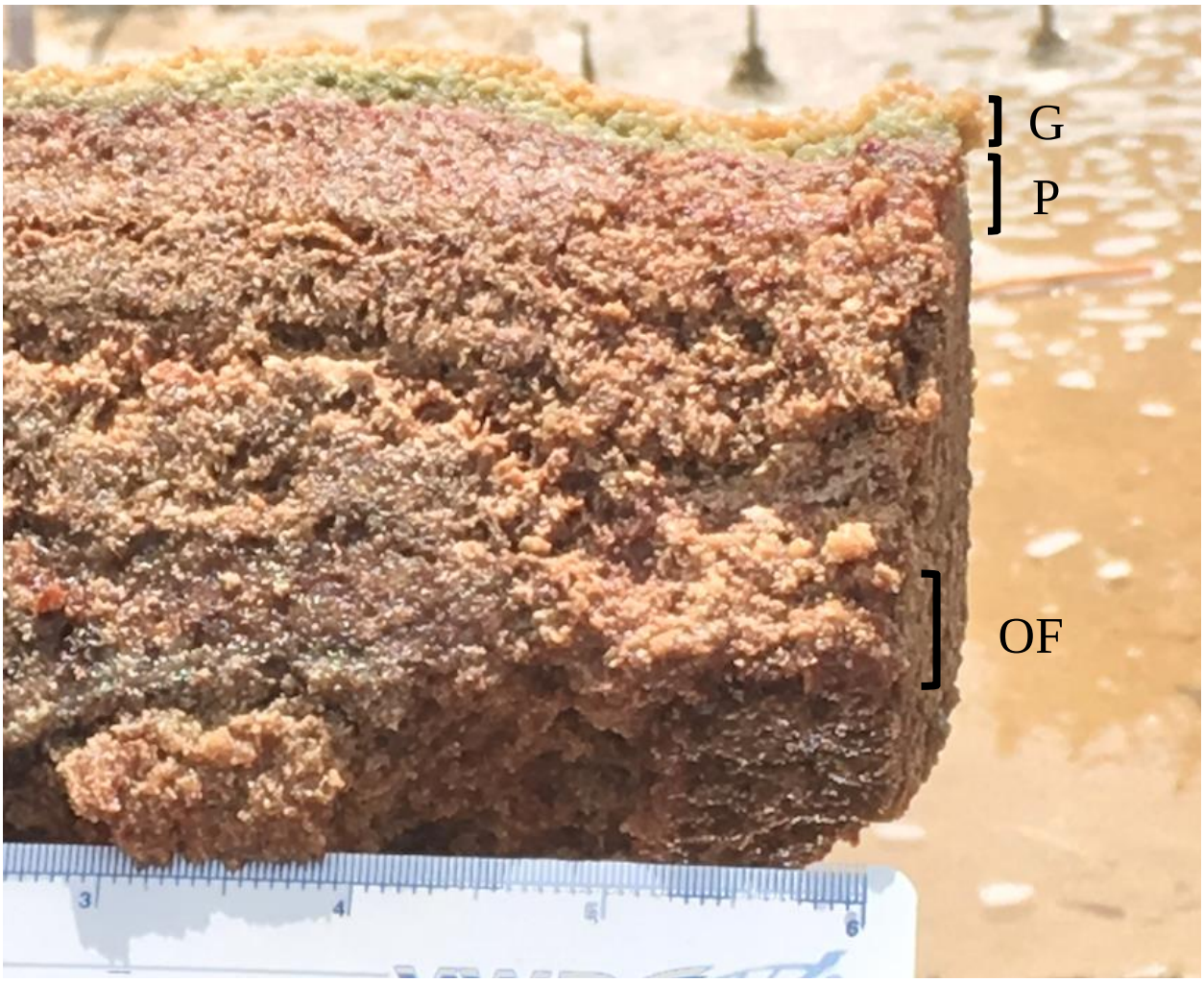

Figure 5. Cross section of flat mat CC3 showing the notable mat layers: G-green, P-pink, OF-old flat mat. The top orange-tan layer is composed of granular EPS. Also note the granular texture of OF. Layers G, P, and OF are the subjects of this study. Photo credit: Maya Gomes.

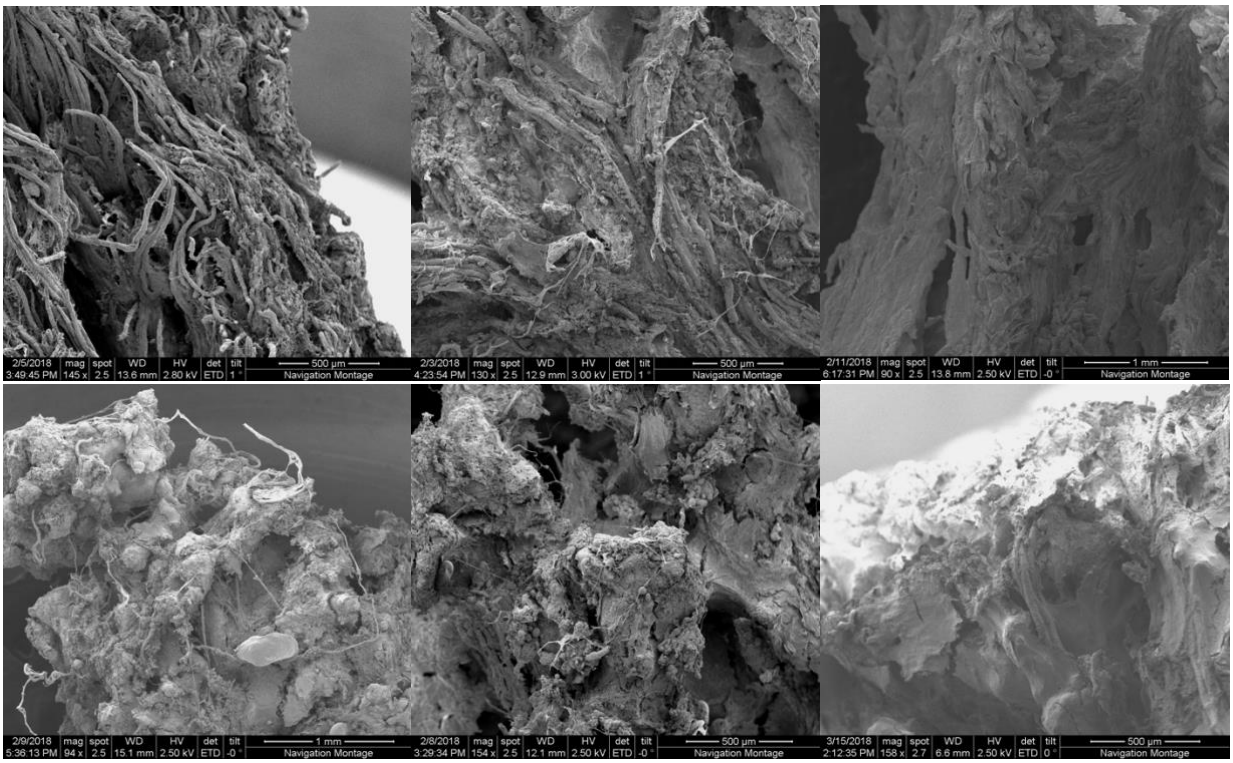

Figure 6. Representative images of the polygonal and flat mats, and their respective layers. From left to right: green layer of the polygonal mat, pink layer of the polygonal mat, old polygonal mat, green layer of the flat mat, pink layer of the flat mat, old flat mat.

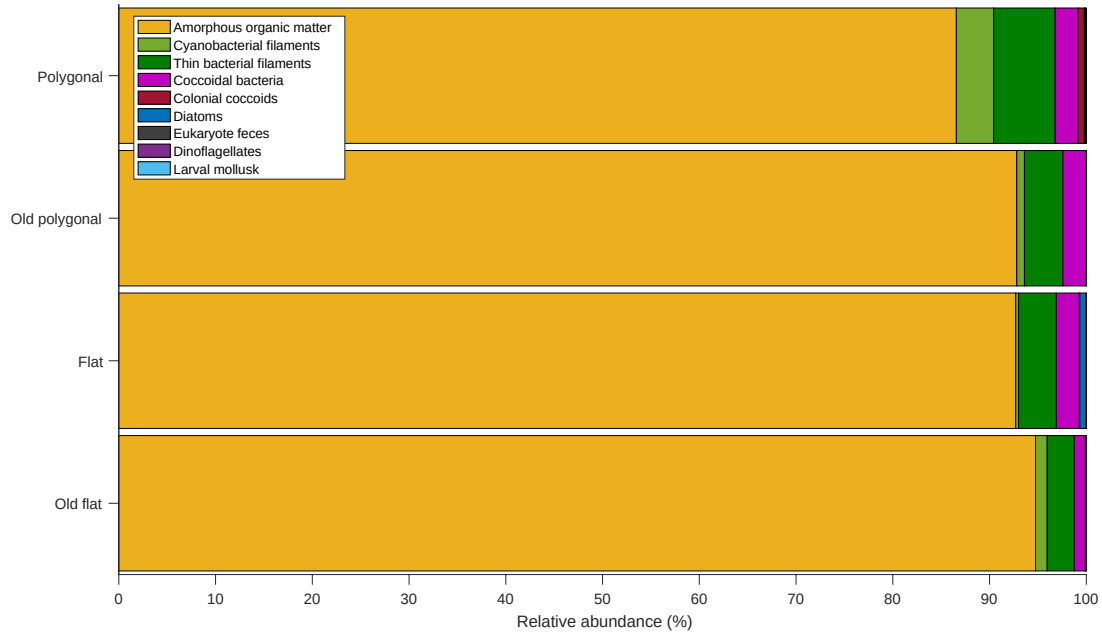

Figure 7. Mat features expressed as percent relative abundance from 100-point counts across twenty sites in the polygonal, flat, old polygonal, and old flat mats. Bars for features with relative abundance <5% are too small to appear. Data in Table A1.

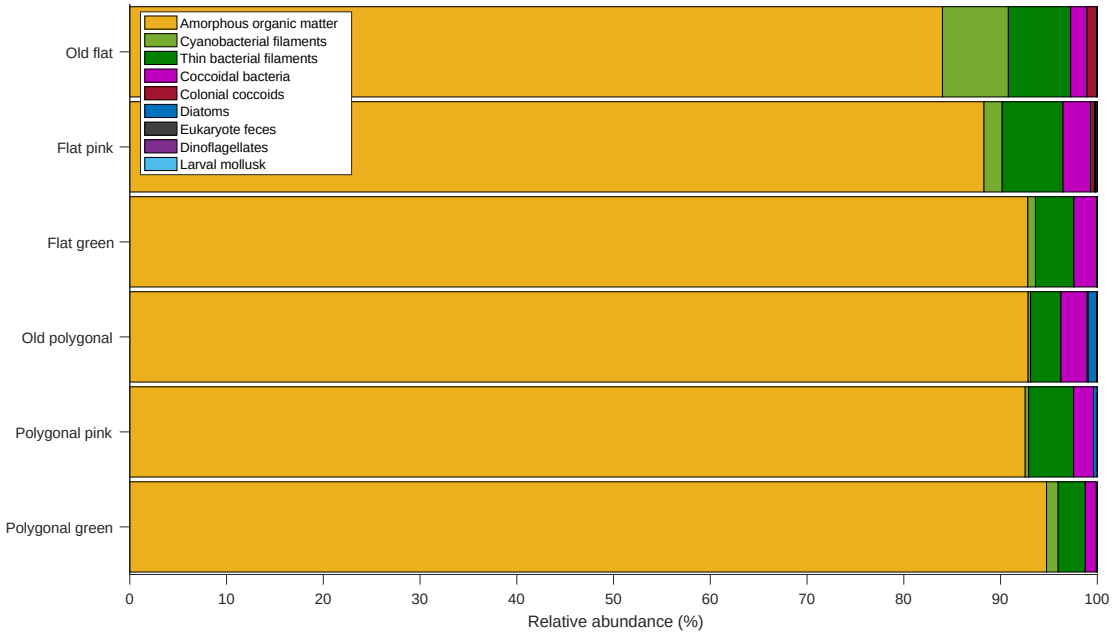

Figure 8. Mat features from the individual mat layers expressed as percent relative abundance from 100-point counts across twenty sites in the polygonal, flat, old polygonal, and old flat mats. Bars for features with relative abundance <5% are too small to appear. Data in Table A1.

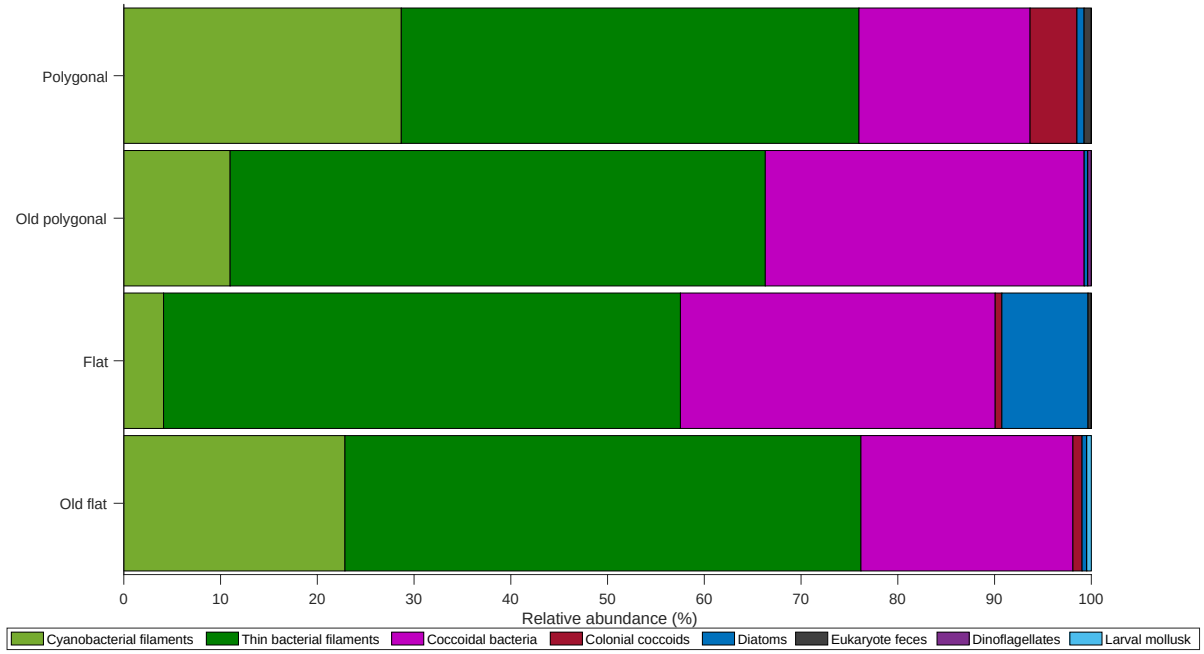

Figure 9. Mat features (without amorphous organic matter) expressed as percent relative abundance from 100-point counts across twenty sites in the polygonal, flat, old polygonal, and old flat mats. Bars for features with relative abundance <5% are too small to appear. Data in Table A1.

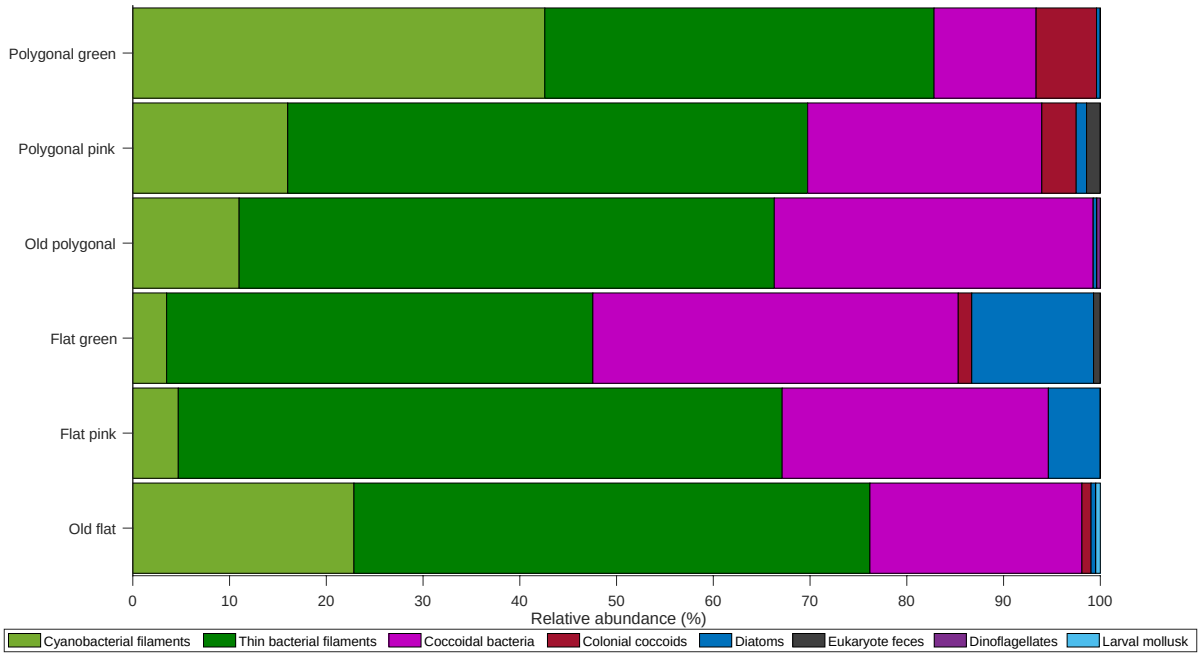

Figure 10. Mat features (without amorphous organic matter) expressed as percent relative abundance from 100-point counts across twenty sites in the polygonal, flat, old polygonal, and old flat mats. Bars for features with relative abundance <5% are too small to appear. Data in Table A1.

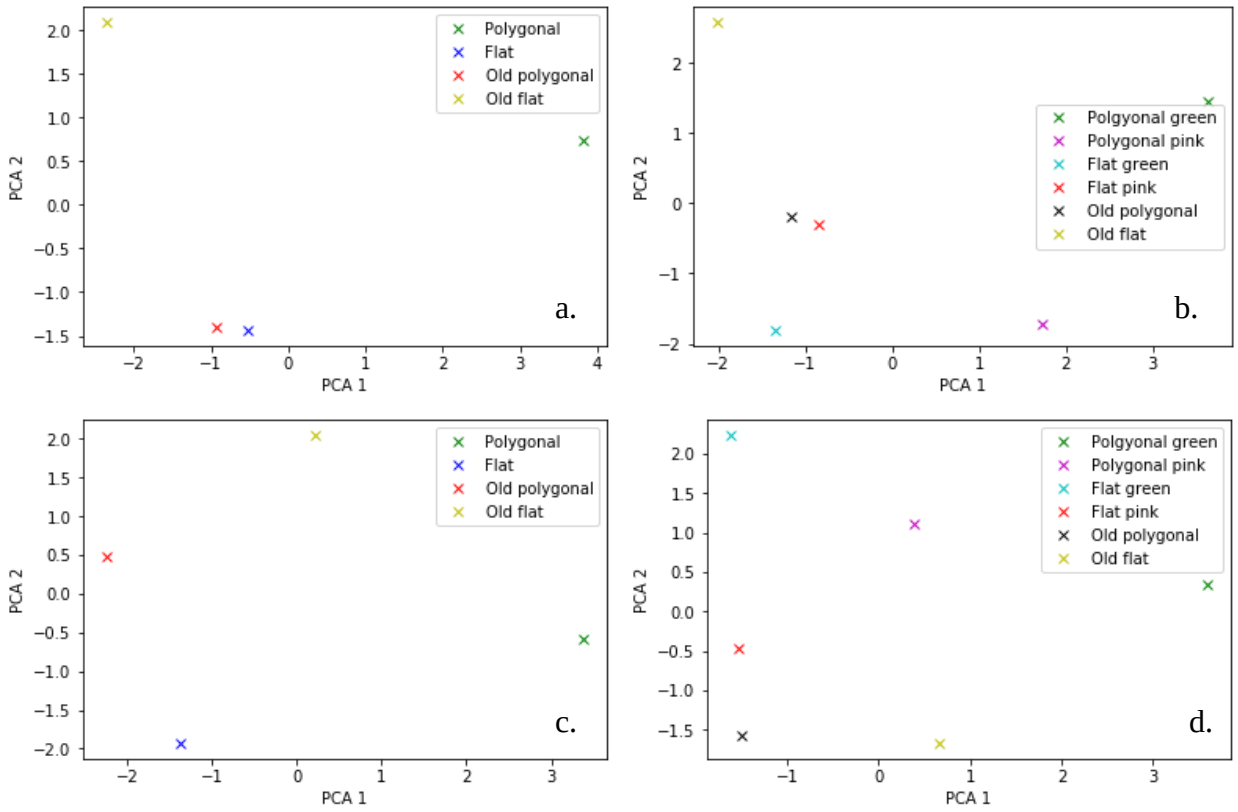

Figure 11. PCA plots of point count data for bulk mats and individual mat layers. Points represent relative abundance data: a,b) with amorphous organic matter, c,d) normalized without amorphous organic matter. Principal components 1 and 2 explain: a) 84% b) 72% c) 85% and d) 68% of the variance.

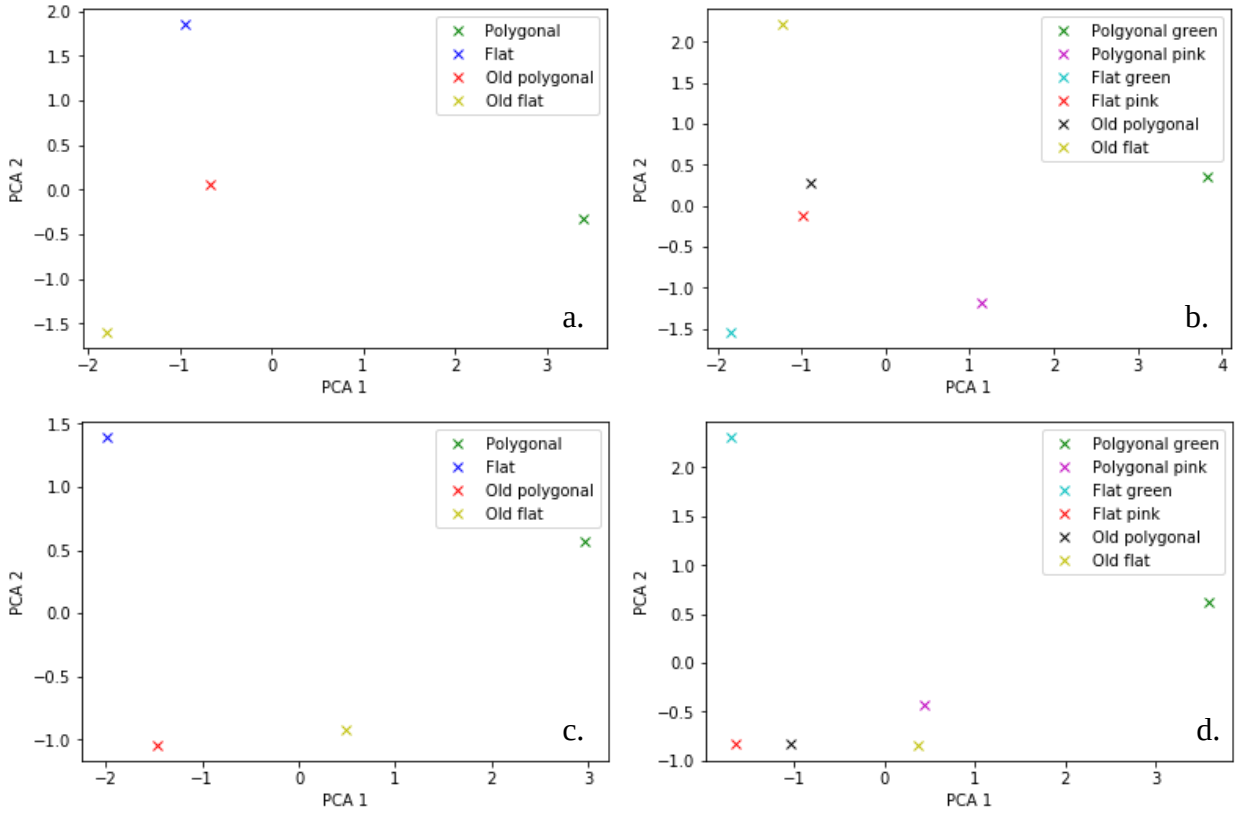

Figure 12. PCA plots of point count data for bulk mats and individual mat layers. Points represent relative abundance data: a,b) with amorphous organic matter, excluding singletons, c,d) without amorphous organic matter, excluding singletons. Principal components 1 and 2 explain: a) 93% b) 88% c) 97% and d) 93% of the variance.

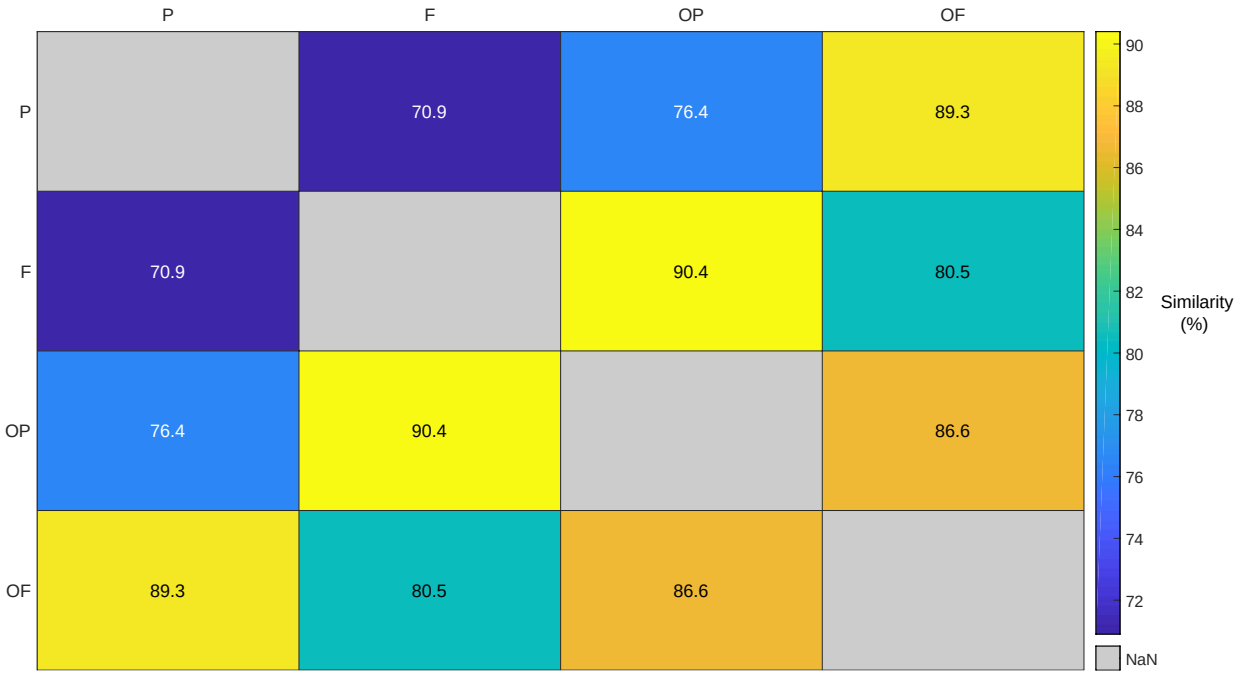

Figure 13. Bray-Curtis similarity matrix for the bulk (green and pink layers) mats. Color scheme indicates percent similarity. P=polygonal mat, F=flat, OP=old polygonal, OF=old flat.

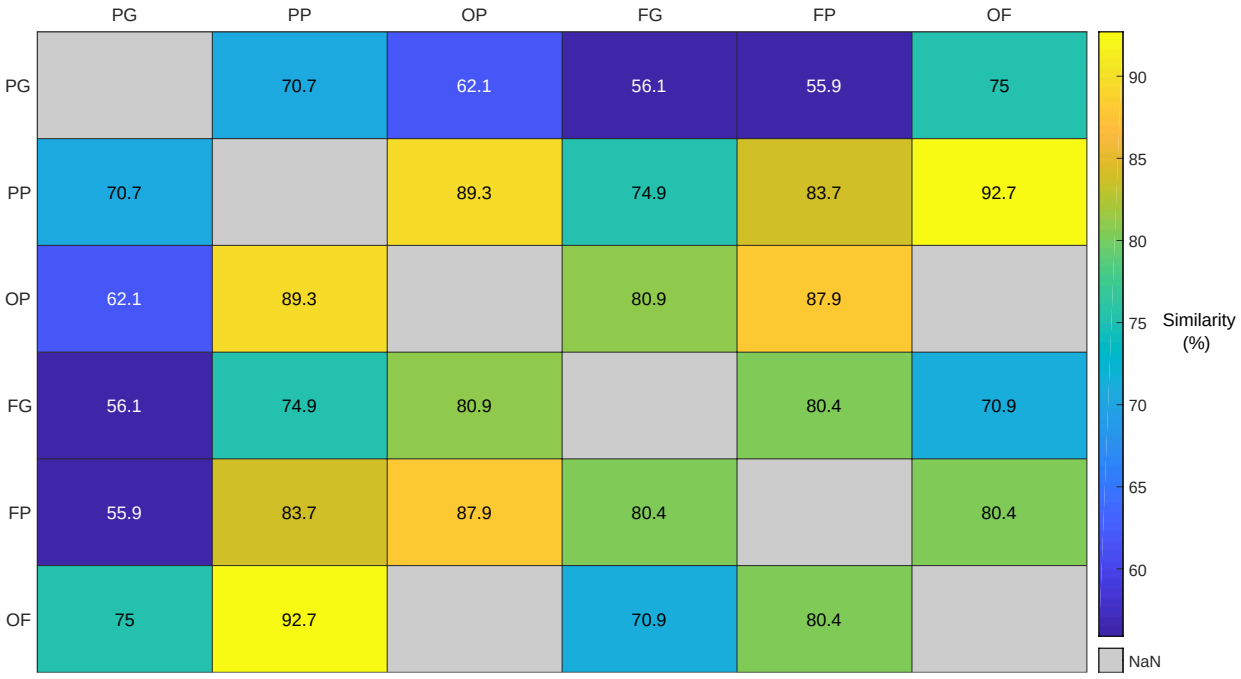

Figure 14. Bray-Curtis similarity matrix for the individual mat layers. PG=polygonal mat green layer, PP=polygonal pink, OP=old polygonal, FG=flat green, FP=flat pink, OF=old flat.

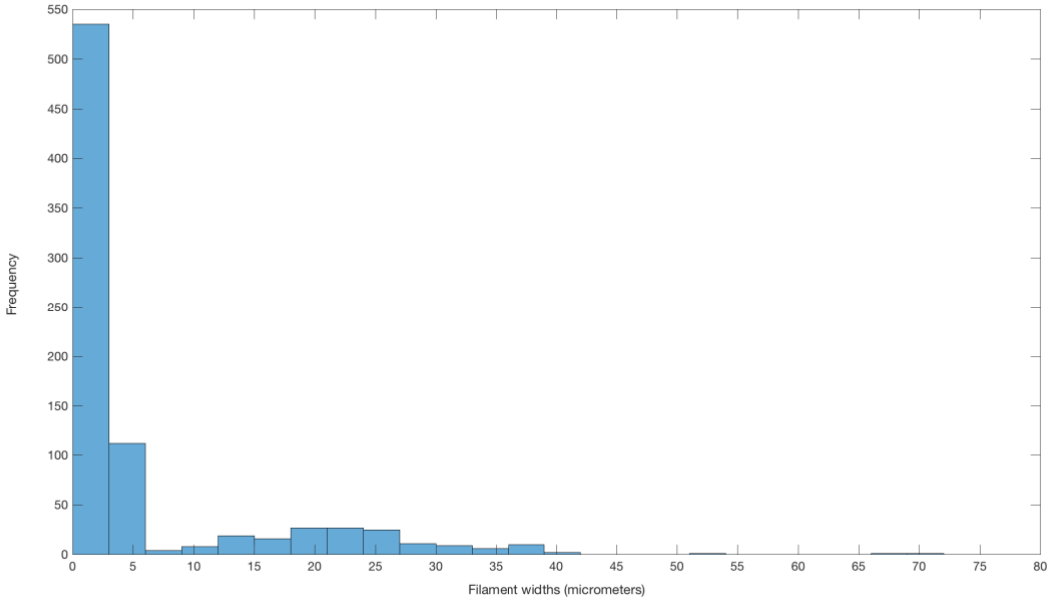

Figure 15. Histogram of filament widths from across all four mat samples. Widths were obtained from bacterial filaments identified during 100-point counts across twenty sites in the polygonal, flat, old polygonal, and old flat mats. Bars for widths greater than 45 micrometers are too small appear in the plot.

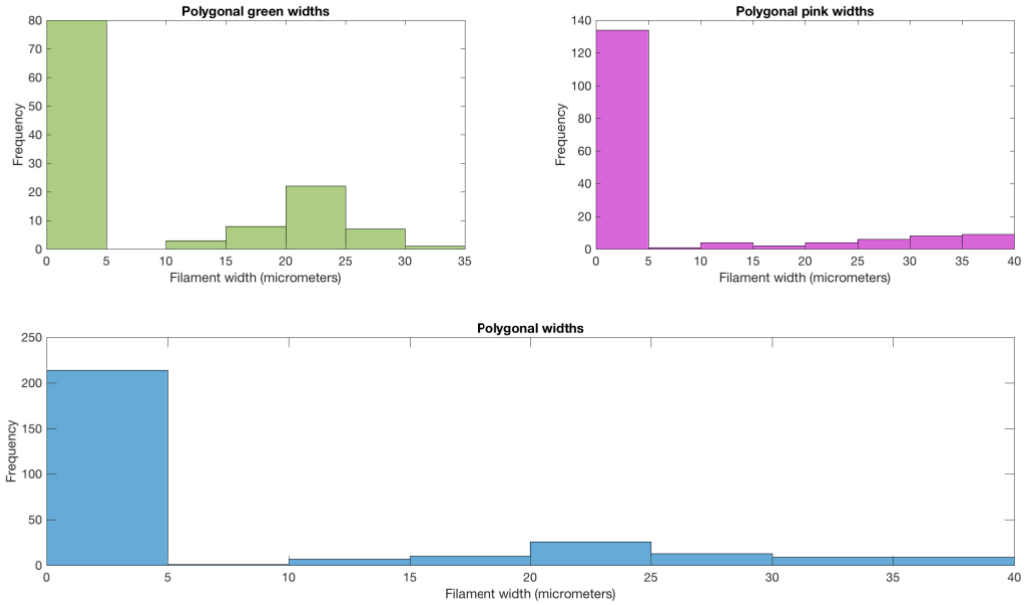

Figure 16. Histograms of filament widths from the green and pink layers of the polygonal mat, and the total filament widths from both layers (bottom panel). Statistical data in Tables A2 and A3.

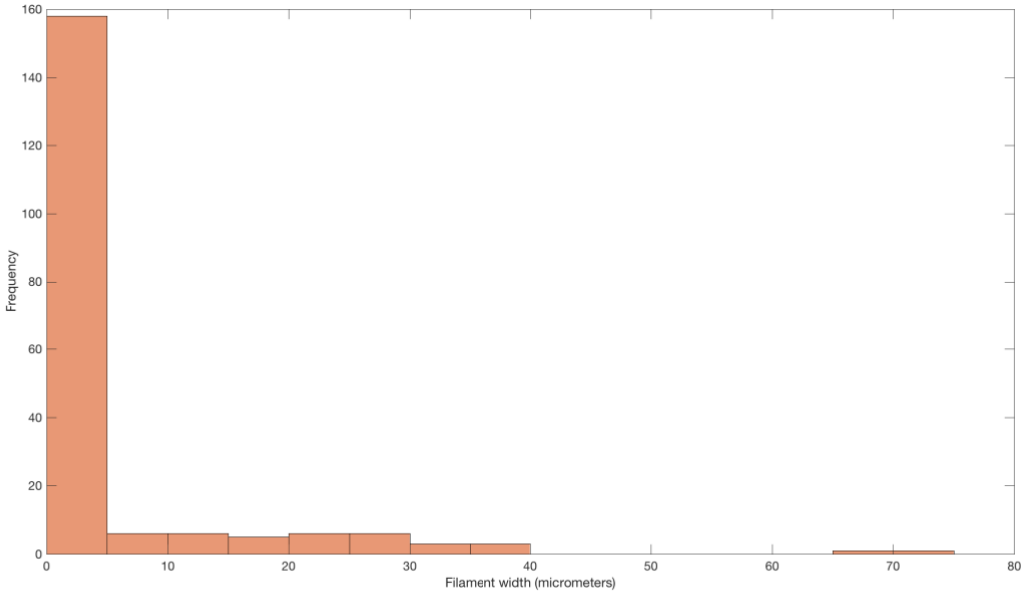

Figure 17. Histogram of filament widths from the old polygonal mat. Statistical data in Tables A2 and A3.

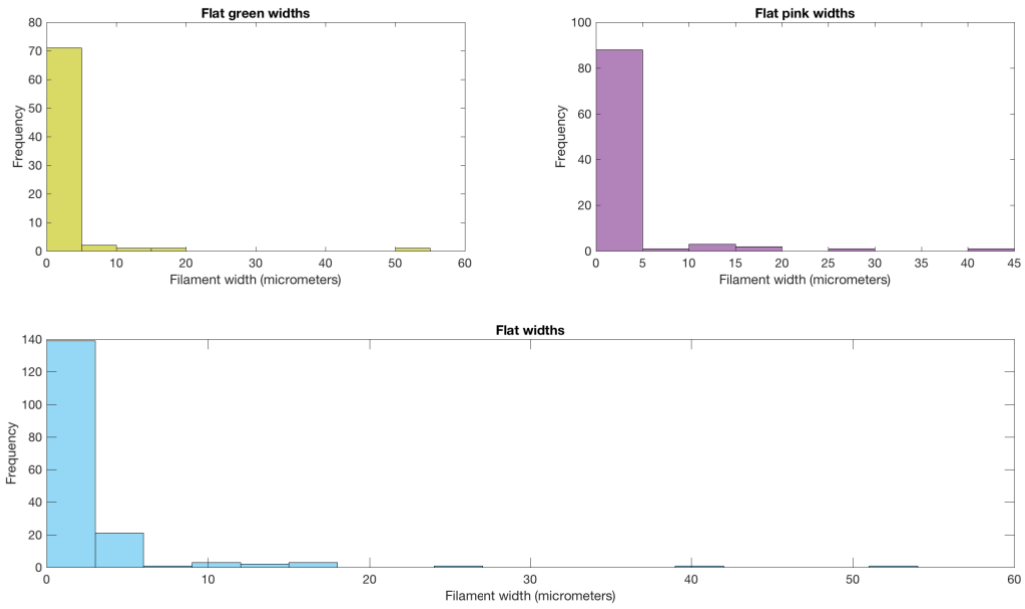

Figure 18. Histograms of filament widths from the green and pink layers of the flat mat, and the total filament widths from both layers (bottom panel). Statistical data in Tables A2 and A3.

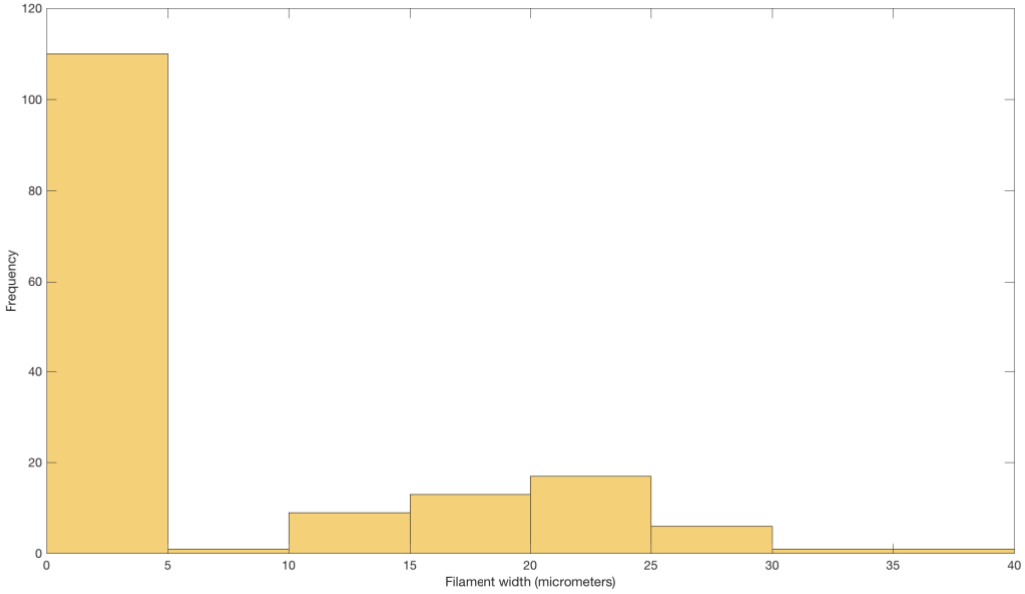

Figure 19. Histogram of filament widths from the old flat mat. Statistical data in Tables A2 and A3.

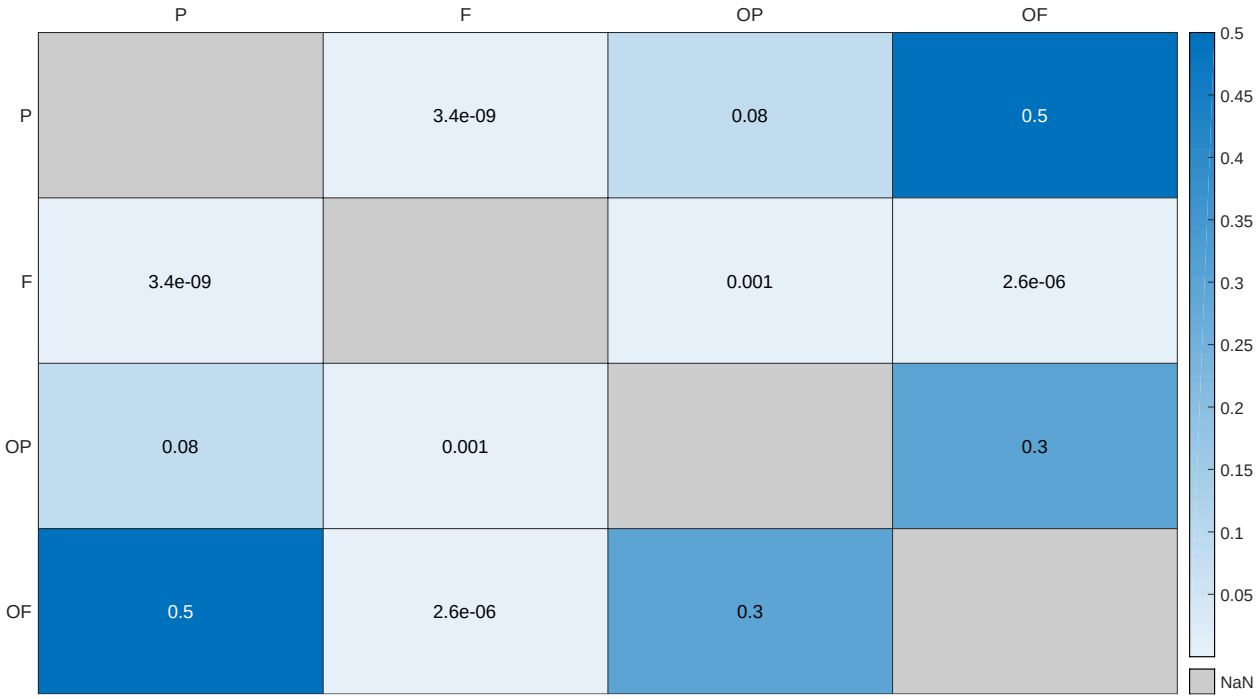

Figure 20. p-value matrix for comparisons of bacterial filament across the entire filament width range of the mats. Higher p-values have darker colors. Significance level is 0.05. P=polygonal, F=flat, OP=old polygonal, OF=old flat. Corresponding T-statistics in Table A4.

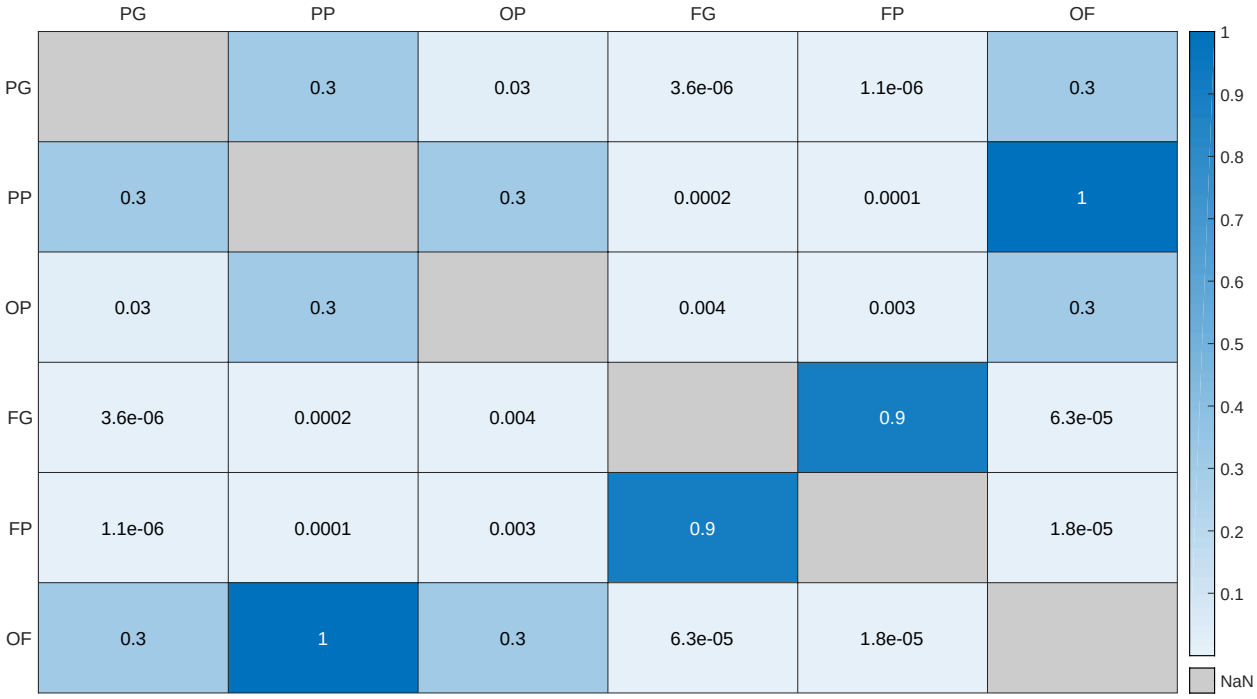

Figure 21. p-value matrix for comparisons of bacterial filament across the entire filament width range of the mats. Higher p-values have darker colors. Significance level is 0.05. PG=polygonal mat green layer, PP=polygonal pink layer, OP=old polygonal, FG= flat green, FP=flat pink, OF=old flat. Corresponding T-statistics in Table A4.

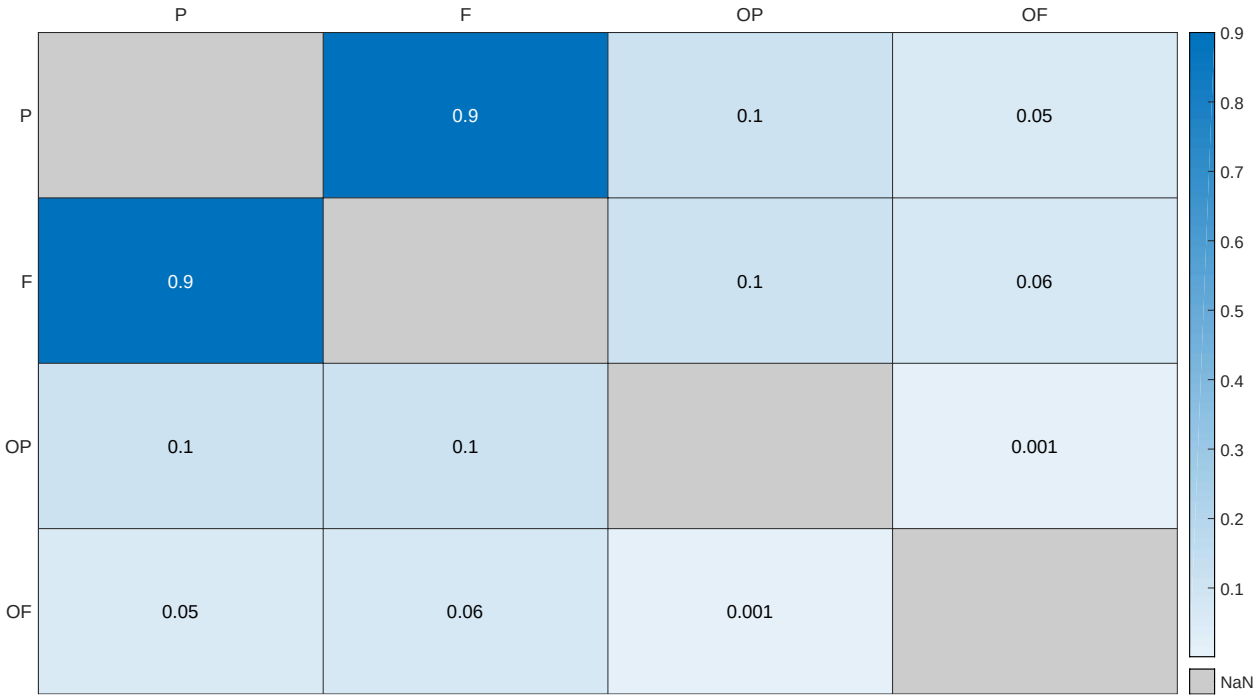

Figure 22. p-value matrix for comparisons of bacterial filament across the filament width range 0-5 µm, where most filament widths occurred. Higher p-values have darker colors. Significance level is 0.05. P=polygonal, F=flat, OP=old polygonal, OF=old flat. Corresponding T-statistics in Table A5.

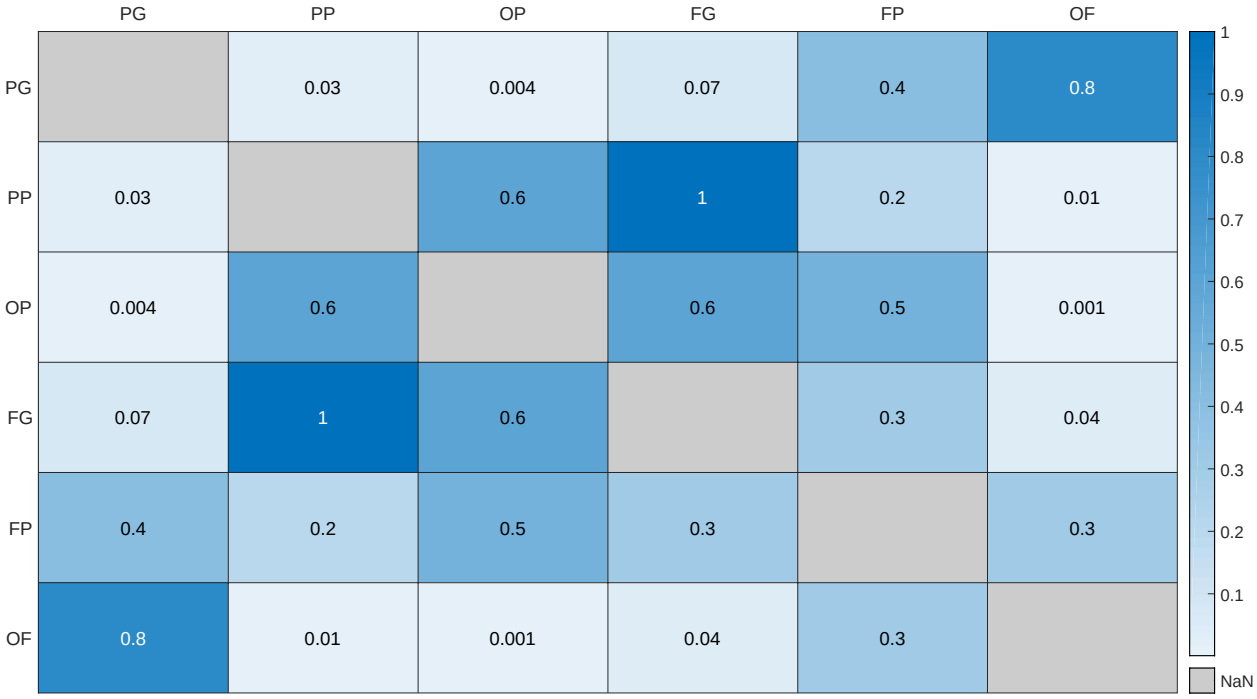

Figure 23. p-value matrix for comparisons of bacterial filament across the filament width range 0-5 µm, where most filament widths occurred. Higher p-values have darker colors. Significance level is 0.05. PG=polygonal mat green layer, PP=polygonal pink layer, OP=old polygonal, FG= flat green, FP=flat pink, OF=old flat. Corresponding T-statistics in Table A5.

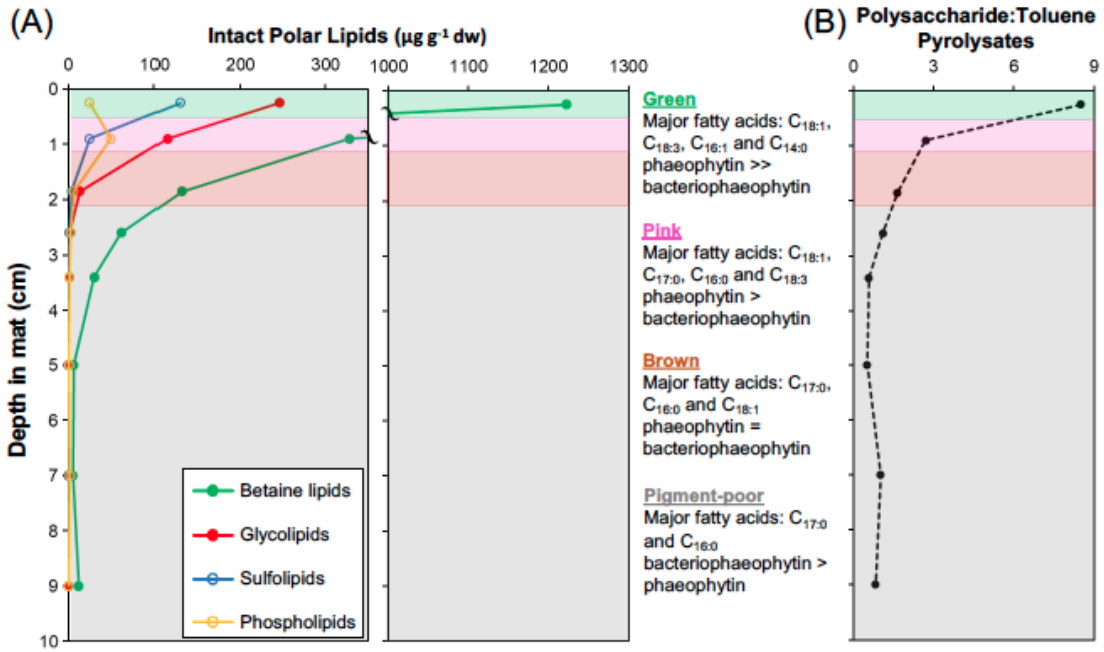

Figure 24. Depth profiles showing the degradation and depletion of labile organic molecules through the green, pink, and brown layers of a polygonal mat from Gomes et al. (*in revision).* Figure used with permission from Gomes et al. (*in revision*).

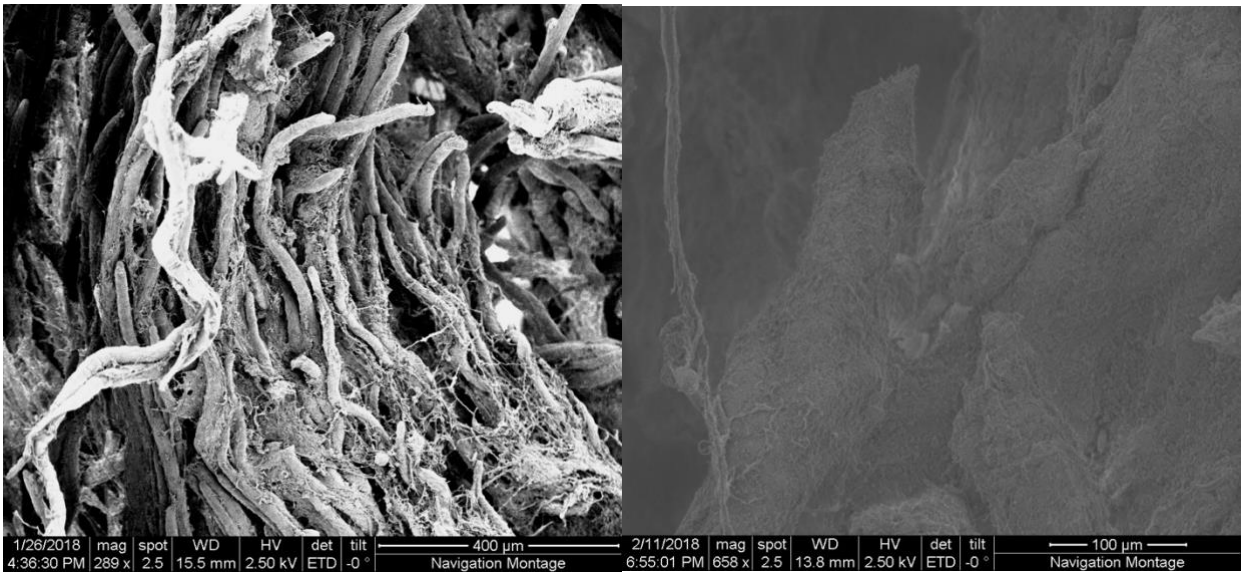

Figure 25. Left: Cyanobacterial filaments from the green layer of the polygonal mat that are not covered in much amorphous organic matter. Right: Thick cyanobacterial filament from the old polygonal mat that is completely covered in amorphous organic matter.

Appendix

Table A1. Absolute abundances of mat features and taxa from point counting.

Feature/Taxa	Polygonal green	Polygonal pink	Flat green	Flat pink	Old polygonal	Old flat
Amorphous organic matter	1343	2118	1856	1851	3526	3790
Cyanobacterial filament	109	45	5	7	30	48
Bacterial filament	103	151	63	93	151	112
Coccoid	27	68	54	41	90	46
Colonial Coccoid	16	10	2	0	0	2
Diatom	1	3	18	8	1	1
Eukaryote feces	0	4	1	0	0	0
Dinoflagellate	0	0	0	0	1	0
Larval mollusk	0	0	0	0	0	1

Table A2. Filament width statistics for mats and their respective layers over the whole filament width range. P=polygonal, F=flat, PG=polygonal green, PP=polygonal pink FG=flat green, FP=flat pink, OP=old polygonal, OF=old flat. Mean widths are reported in micrometers and n is number of filaments measured.

	P	PG	PP	F	FG	FP	OP	OF
n	289	121	168	172	76	96	195	158
Mean	7.9	8.6	7.4	3.3	3.2	3.3	6.2	7.3
Standard deviation	10.6	9.8	11.2	5.8	6.1	5.5	10.4	8.9
Variance	113.0	95.3	125.1	33.3	37.5	30.0	107.1	79.8

Table A3. Filament width statistics for mats and their respective layers for the filament width range 0-5 μm. P=polygonal, F=flat, PG=polygonal green, PP=polygonal pink FG=flat green, FP=flat pink, OP=old polygonal, OF=old flat. Mean widths are reported in micrometers and n is number of filaments measured.

	P	PG	PP	F	FG	FP	OP	OF
n	214	80	134	159	71	88	158	110
Mean	2.0	1.8	2.1	2.0	2.1	2.0	2.2	1.8
Standard deviation	1.0	0.8	1.1	1.0	1.1	0.9	1.1	0.8
Variance	1.0	0.6	1.1	0.9	1.2	0.8	1.2	0.7

Table A4. T-statistics from Welch's t-test. Tests cover whole filament width range. P=polygonal, F=flat, PG=polygonal green, PP=polygonal pink, FG=flat green, FP=flat pink, OP=old polygonal, OF=old flat.

Comparison	T-statistic
P-F	6.0
OP-P	-1.8
OF-P	-0.6
OP-F	3.3
OF-F	4.8
OP-OF	1.1
PG-PP	1.0
PG-FG	4.8
PG-FP	5.0
PP-FP	3.9
PP-FG	3.7
FG-FP	-0.15
OF-FG	4.1
OF-FP	4.4
OF-PG	1.2
OF-PP	-0.06
OP-FG	2.9
OP-FP	3.0
OP-PG	-2.1
OP-PP	-1.1

Table A5. T-statistics from Welch's t-test. Tests cover filament width range 0-5 μm. P=polygonal, F=flat, PG=polygonal green, PP=polygonal pink, FG=flat green, FP=flat pink, OP=old polygonal, OF=old flat.

Comparison	T-statistic
P-F	-0.08
OP-P	-1.7
OF-P	2.0
OP-F	-1.5
OF-F	1.9
OP-OF	3.3
PG-PP	-2.3
PG-FG	-1.8
PG-FP	-0.9
PP-FP	1.4
PP-FG	0.02
FG-FP	1.1
OF-FG	-2.1
OF-FP	-1.1
OF-PG	-0.2
OF-PP	-2.6
OP-FG	0.5

OP-FP	2.0
OP-PG	2.9
OP-PP	0.6

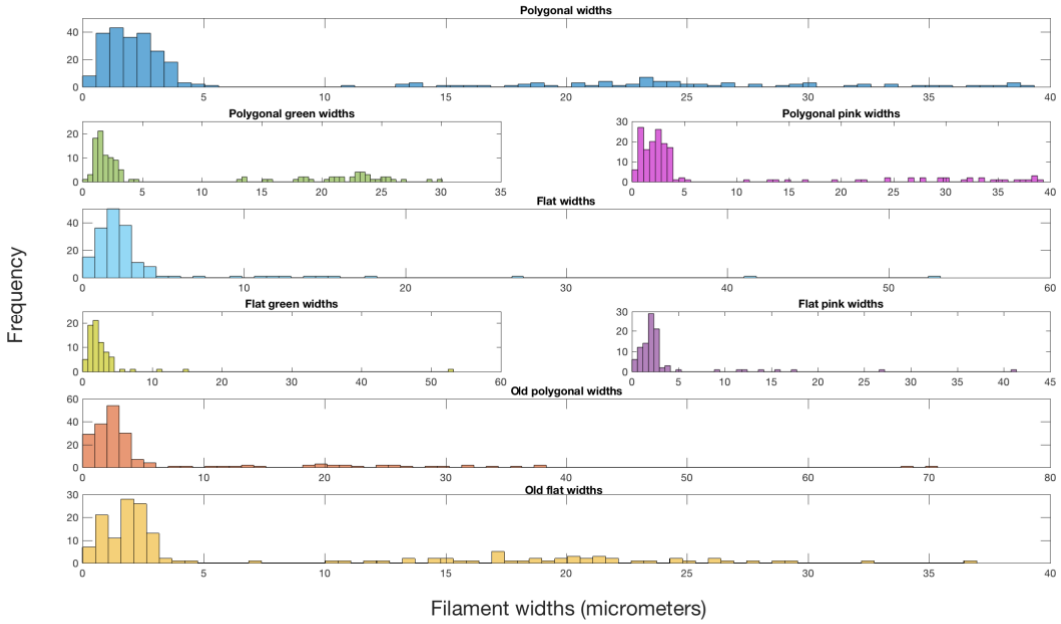

Figure A1. Histograms of filament widths from all mat types and layers. The bin number (70) was chosen to show the filament width distributions at a higher resolution than those in Figures 15-19.